DOI: 10.1534/genetics.110.120790

Genetic and Epigenetic Dynamics of a Retrotransposon After Allopolyploidization of Wheat

Zina Kraitshtein,[1] Beery Yaakov,[1] Vadim Khasdan and Khalil Kashkush[2]

Department of Life Sciences, Ben-Gurion University, Beer-Sheva 84105, Israel

Manuscript received July 10, 2010
Accepted for publication September 6, 2010

ABSTRACT

Allopolyploidy, or the combination of two or more distinct genomes in one nucleus, is usually accompanied by radical genomic changes involving transposable elements (TEs). The dynamics of TEs after an allopolyploidization event are poorly understood. In this study, we analyzed the methylation state and genetic rearrangements of a high copied, newly amplified terminal-repeat retrotransposon in miniature (TRIM) family in wheat termed *Veju*. We found that *Veju* insertion sites underwent massive methylation changes in the first four generations of a newly formed wheat allohexaploid. Hypomethylation or hypermethylation occurred in ~43% of the tested insertion sites; while hypomethylation was significantly predominant in the first three generations of the newly formed allohexaploid, hypermethylation became predominant in the subsequent generation. In addition, we determined that the methylation state of *Veju* long terminal repeats (LTRs) might be correlated with the deletion and/or insertion of the TE. While most of the methylation changes and deletions of *Veju* occurred in the first generation of the newly formed allohexaploid, most *Veju* insertions were seen in the second generation. Finally, using quantitative PCR, we quantitatively assessed the genome composition of *Veju* in the newly formed allohexaploid and found that up to 50% of *Veju* LTRs were deleted in the first generation. Retrotransposition bursts in subsequent generations, however, led to increases in *Veju* elements. In light of these findings, the underlying mechanisms of TRIM rearrangements are discussed.

TRANSPOSABLE elements (TEs) are DNA sequences that range in size from several hundred base pairs to >15 kb and that have the ability to move to different locations within the genome. TE movement occurs through either a copy-and-paste mechanism involving RNA intermediates (class 1) or a cut-and-paste mechanism involving DNA intermediates (class 2). Class 1 elements are also called retrotransposons, or retroelements, and comprise two main types: (1) long terminal repeat (LTR) retrotransposons, flanked by LTRs, and (2) non-LTR elements (such as long interspersed nuclear elements and short interspersed nuclear elements).

LTR retrotransposons are the most abundant mobile elements in plant genomes (Feschotte *et al.* 2002), as the replicative mode of retroelement transposition enables the LTR retrotransposon to accrue in high copy number. Indeed, in some grasses, LTR retrotransposons represent up to 90% of the genome (Bennetzen and Kellogg 1997; Feschotte *et al.* 2002). As such, retrotransposon sequences function well as substrates for illegitimate and unequal recombinations that can lead to a variety of mutations, such as deletions, insertions, translocations, and others (Parisod *et al.* 2009).

The replicative nature of TEs seems to be stimulated by a variety of specific stress conditions (reviewed by Wessler 1996; Capy *et al.* 2000; Grandbastien *et al.* 2005), including challenges to the genome such as interspecific hybridization, an idea first proposed by Barbara McClintock 26 years ago (McClintock 1984). Accordingly, allopolyploidization is usually coupled with rapid and reproducible genomic changes, including the elimination of DNA sequences (Liu *et al.* 1998a,b; Ozkan *et al.* 2001; Shaked *et al.* 2001; Adams and Wendel 2005b; Skalicka *et al.* 2005), gene silencing (Chen and Pikaard 1997; Comai *et al.* 2000; Kashkush *et al.* 2002; Simons *et al.* 2006), alteration of cytosine methylation (Shaked *et al.* 2001; Madlung *et al.* 2002; Salmon *et al.* 2005; Beaulieu *et al.* 2009; Xu *et al.* 2009), activation of genes and retrotransposons (Kashkush *et al.* 2002, 2003; O'Neill *et al.* 2002), massively altered gene expression patterns (Kashkush *et al.* 2002; Wang *et al.* 2006), and organ-specific subfunctionalization, *i.e.*, differential expression of homeoalleles in different tissues and at different developmental stages (Adams *et al.* 2003; Adams and Wendel 2004). These and other studies (Levy and Feldman 2002; Osborn *et al.* 2003; Adams and Wendel 2005a; Rapp and Wendel 2005; Chen and Ni 2006; Chen 2007) demonstrate the dynamic nature of allopolyploid plant genomes.

Supporting information is available online at http://www.genetics.org/cgi/content/full/genetics.110.120790/DC1.

[1]These authors contributed equally to this work.

[2]*Corresponding author:* Department of Life Sciences, Ben-Gurion University, Beer-Sheva 84105, Israel. E-mail: kashkush@bgu.ac.il

Although allopolyploidization has generally been assumed to induce large bursts of TE activity (Matzke and Matzke 1998), several studies that focused on different allopolyploid systems failed to provide any evidence for a transposition burst and offered only limited evidence for the transposition of specific TEs (Madlung *et al.* 2005; Ainouche *et al.* 2009; Beaulieu *et al.* 2009). In newly formed Arabidopsis allopolyploids, no evidence for transposition bursts was reported (Beaulieu *et al.* 2009), although limited evidence suggested that transposition events occurred in a specific TE called *Sunfish* (Madlung *et al.* 2005). Little evidence of TE transposition was found in a natural population of the 150-year-old allopolyploid, *Spartina anglica* (Ainouche *et al.* 2009), and no evidence of transposition of *Wis 2-1A* retrotransposons in a newly formed wheat allotetraploid was present (Kashkush *et al.* 2003). The results of these works and others indicate that, in the short term, TE proliferation after allopolyploidization may be restricted to a few specific TEs in particular allopolyploidy systems (Parisod *et al.* 2009).

This study entailed a detailed investigation of the methylation patterns and rearrangements of a one terminal-repeat retrotransposon in miniature (TRIM) family in wheat termed *Veju*. TRIM elements possess the classical structure of LTR retrotransposons, but they are distinguished by their small overall sizes (0.4 to ~2.5 kb). A nonautonomous retrotransposon, *Veju* is 2520 bp long with 374 bp of identical LTRs, yet does not contain the proteins required for retrotransposition (Sanmiguel *et al.* 2002). However, because *Veju* elements contain polypurine tracts (PPTs) and primer binding sites (PBSs), they are capable of transposing if the retrotransposition proteins are available from another source. In addition, the identical sequences of the *Veju* 5′ and 3′ LTRs indicate that some members of the *Veju* family retain retrotransposition activity.

In silico analysis of *Veju* sequences revealed them to be one of the most active and most recently inserted sequences in the wheat genome (Sanmiguel *et al.* 2002; Sabot *et al.* 2005a). As such, we have determined and compared the methylation patterns of >880 *Veju* insertion sites in the first four generations of a newly formed wheat allohexaploid, as well as in the parental lines. We then tested the correlation between the cytosine methylation and genetic rearrangements (*i.e.*, deletions and insertions) of *Veju* and addressed the precise developmental timing of these rearrangements. Finally, we successfully tested overall changes in the copy numbers of *Veju* in the newly formed allohexaploid using real-time quantitative PCR.

MATERIALS AND METHODS

Plant material: The plant material used in this study comprised a newly formed allohexaploid (S1–S5 generations) and the parental lines *Triticum turgidum* ssp. *durum* (accession no. TTR19) and *Aegilops tauschii* (accession no. TQ27). The amphiploid was obtained through the spontaneous formation of unreduced gametes in F_1 plants (Ozkan *et al.* 2001). Chromosome number was determined in newly formed allohexaploids, and only those having the expected euploid chromosome number were analyzed. Seed materials from the parental lines, S1, and S2 were kindly provided by Hakan Ozkan and Moshe Feldman.

DNA isolation: DNA was isolated from young leaves (4 weeks post germination) using the CTAB technique (Kidwell and Osborn 1992) or the DNeasy plant kit (QIAGEN). In addition, DNA was isolated from various tissues of S1 and S2 plants (see details in results).

Transposon methylation display and transposon display: DNA isolated from newly formed allohexaploids and the parental lines was subjected to transposon methylation display (TMD) according to a previously published protocol (Kashkush and Khasdan 2007). *Veju*-specific primers from the 5′ LTR (P2 in Table S1) and from the 3′ LTR (P3 in Table S1) were used in the TMD together with an adapter primer, + (TCAG) (Figure 1, P1) (see Kashkush and Khasdan 2007). Primer positions in the *Veju* sequence are displayed in Figure S1. The fluorescently labeled TMDs were analyzed by GeneMapper version 4 (see examples in Figure S2). Chimeric (*Veju*/host flanking sequence) TMD bands with evidence of alteration (loss/gain of bands) between newly formed allopolyploid generations and/or their parents were extracted from the polyacrylamide gel, reamplified (using the same PCR conditions as in the preamplification reaction for TMD), cloned, and sequenced.

Transposon display (TD) was performed using a methylation-insensitive restriction enzyme, *Mse*I with an adaptor primer, + (CAC, CTG, or CAT) (Table S1), together with a *Veju*-specific primer from the 5′ LTR (P2 in Table S1).

Site-specific PCR: All PCR reactions were performed with 2 μl Taq DNA polymerase buffer 10× (Fisher Biotec), 2.0 μl of 25 mm $MgCl_2$ (Fisher Biotec), 0.8 μl 2.5 mm dNTPs, 0.2–0.3 μl of Taq DNA polymerase (5000 units/ml, Fisher Biotec), 1 μl of forward primer (50 ng/μl), 1 μl of reverse primer (50 ng/μl), and 25–100 ng DNA template, to which ultra-pure, double-distilled water was added to achieve a final volume of 20 μl. PCR conditions were 94° for 3 min followed by a cycling stage of denaturation at 94° for 30 sec, annealing for 30 sec, and elongation at 72° for 30–70 sec, repeated for 29 cycles. Primers were designed using Primer 3 software version 0.4.0 (http://frodo.wi.mit.edu/primer3/input.htm). Ultra-pure double-distilled water served as template in all negative control PCR reactions. PCR products were visualized on 1.5–2% agarose gel using TAE buffer (40 mm Tris base, 0.1% HCl, and 1 mm EDTA, pH 8) under UV light after staining with ethidium bromide. The primer sequences used for genomic PCR amplifications are described in Table S1.

Quantitative PCR: Primers for PCR were designed using the online program Primer 3 (version 0.4.0) and verified using Primer Express software version 3.0 (Applied Biosystems). Each quantitative PCR (qPCR) reaction was performed in a 15-μl reaction volume that consisted of 7.5 μl of Power SYBR Green PCR reaction mix 2× (Applied Biosystems), 5 μl of DNA template (0.5 ng/μl), 1 μl of forward primer (10 μm), 1 μl of reverse primer (10 μm), and 0.5 μl of ultra-pure water. The qPCR reactions were performed and analyzed using the 7500 Fast Real-Time PCR system and 7500 Software version 2.0.1 (Applied Biosystems), respectively. The thermal profile consisted of 2 min at 50°, 10 min at 95°, and 40 cycles of 4 sec at 95° and 30 sec at 60°. Amplification data were collected at the end of each extension step. Primer sequences used for qPCR amplifications are described in Table S2. The ratio of *Veju* LTRs to internal region sequences was calculated using the following

formula: ratio = (the fold of template amplification at each cycle)$^{-\text{average }\Delta Ct}$, where ΔCt (threshold cycle) = $Ct_{(target)} - Ct_{(reference\ control)}$. *Veju* LTR was set as the target, and the internal region of *Veju* served as a reference.

A comparative $2^{-\Delta\Delta Ct}$ method for determining a relative target quantity in samples was used in the normalization and analysis of the relative quantities of both the LTR and the internal *Veju* sequences. Using 7500 software version 2.0.1, we measured amplification of the target—either the *Veju* LTR or the internal region—and of the endogenous control of *VRN1* in samples and in a reference sample (in this case the diploid parental line is TQ27). The same software was then used to determine the relative quantity of target in each sample by comparing the normalized target quantity in each sample to the normalized target quantity in the reference sample, TQ27, based on the following equation:

$$\Delta\Delta Ct_{(\text{test sample})} = \left[Ct_{(target)} - Ct_{(VRN1)}\right]_{\text{test sample}} - \left[Ct_{(target)} - Ct_{(VRN1)}\right]_{TQ27}.$$

Therefore, the relative quantity = (the fold of template amplification at each cycle)$^{-\Delta\Delta Ct}$ (Livak and Schmittgen 2001).

Reproducibility of the results was evaluated for each sample by running three technical replicates of each of the reactions. To ensure experimental reproducibility, three biological replicates were run for each genotype. To distinguish specific from nonspecific PCR products, a melting curve was generated immediately after amplification. It consisted of a 15-sec incubation at 95° and a 1-min incubation at 60°, after which the temperature was increased by increments of 0.1°/sec until 95° was reached. The same specific product was detected for either target or reference genes, while no amplification was detected in the no-template control wells.

PCR efficiencies of the target and reference genes were determined by generating standard curves, based on serial dilutions prepared from DNA templates. Fold amplification at each cycle was calculated according to PCR efficiency, which was deduced by the software from the slope of the regression line (y) according to the equation $E = [(10^{-1/y}) - 1] \times 100$. For primers with 100% efficiency, the fold equals 2. For other efficiencies, the software adjusts the fold accordingly (Table S2).

Computer-assisted analysis: Sequence annotation relied on the BLAST 2.0 package from the National Center for Biotechnology Information (http://www.ncbi.nlm.nih.gov/BLAST/) and from the Institute for Genomic Research (http://tigrblast.tigr.org/tgi/).

RESULTS

Defining the methylation status of *Veju* LTR-flanking sequences in newly formed allohexaploids and in the parental lines: The methylation status of *Veju* LTR-flanking CCGG sites in the two parental lines *T. turgidum* (TTR19) and *A. tauschii* (TQ27) and in the first four generations (S1–S4) of the derived allohexaploid (see materials and methods, *Plant material*) was investigated using transposon methylation display. TMD enables systematic, genome-wide analysis of the methylation status of CCGG sites in DNA that flanks high-copy-number TEs (Kashkush and Khasdan 2007). Gel-based analysis of the TMD products revealed that each TMD band contains a *Veju* LTR sequence at one end and an unmethylated *Hpa*II (H) or *Msp*I (M) site in the flanking sequences (Figure 1 and Figure S2). Note that because the two *Veju* LTRs are nearly identical, *Veju* internal sequences theoretically might also be amplified when a *Veju* LTR primer (P2) is used in a TMD reaction (see Figure S1), which thereby enables the analysis of the methylation status also in CCGG sites within *Veju* internal sequence. However, no such bands were identified in our analysis. The appearance of monomorphic bands (present in both the H and M lanes of the same individual) in the TMD gel indicates that no methylation was detected at the CCGG site flanking the LTR. However, the presence of polymorphic bands indicates the presence of methylation either at an internal cytosine residue (bands present in M lanes only) or at an external cytosine residue (bands present in H lanes only, reflecting hemi-methylation) of the CCGG site flanking the LTR. Using TMD, we analyzed 889 clear bands (*Veju* insertion sites) in the parental lines (559 and 330 bands in TTR19 and TQ27, respectively). Monomorphic bands in TMD gels in the two parental lines (which indicate similar insertions in the parents) were counted only once, and 207 such bands were counted. Of the 889 bands analyzed, 361 were polymorphic between the H and M lanes, indicating that 40.6% (361/889) of the CCGG sites flanking *Veju* LTRs were methylated in the DNA isolated from young leaves of the parental lines. The two parental lines, TTR19 and TQ27, showed similar levels of methylation, namely 41.3% and 40%, respectively (Table S3).

We expected all TMD bands to be inherited, reflecting additivity in the newly formed allohexaploid generations (*i.e.*, the S generations) because both parents derived from inbred lines (Ozkan *et al.* 2001). Deviations from additivity (revealed as a loss or a gain of a band) in any of the S generations may be due to methylation alterations, deletions, and/or insertions. When the inheritance of the TMD bands (loci) was tested, 486 of the 889 (54.6%) TMD bands were altered in the first four generations (S1–S4). Hence, in summary, alterations of TMD patterns (Table 1) in the S generations can be classified into five groups (examples of TMD patterns representing the five groups are shown in Table S4):

1. Clear, detectable alterations in the methylation of *Veju* LTR-flanking CCGG sites in S1–S4 accounted for 65.6% of the changes (319 bands, Table 1). Hypomethylation (release of methyl groups from one or both cytosines at CCGG sites that were methylated in one or both parental lines) or hypermethylation (gain of methyl groups on CCGG sites that were unmethylated at one or both cytosines in one or both parental lines) had occurred already in S1. Although hypomethylation occurred for ~80% of the cases in S1, it decreased in subsequent generations to reach ~30% in S4 (Figure 2A).
2. Absence of bands in S1 had already occurred for ~6% (31 bands, Table 1) of the TMD changes.

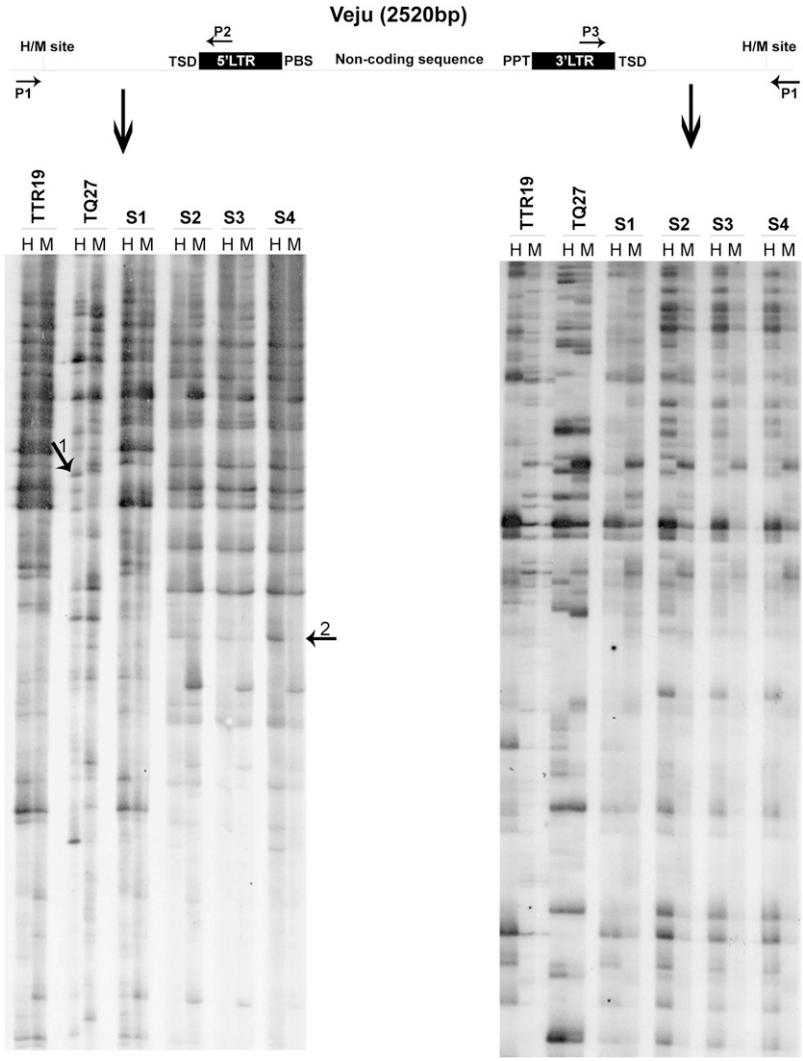

FIGURE 1.—TMD patterns in *T. turgidum* ssp. *durum* (TTR19) and *Ae. tauschii* (TQ27) and in the first four generations (S1–S4) of the derived allohexaploid. *Veju* and its flanking sequences are shown (scheme at the top) together with *Hpa*II (H) and *Msp*I (M) cleavage sites and the positions of primers used in TMD reactions. Autoradiographs of TMD used P2 or P3 and the adapter primer (P1), +(TCAG). Primer sequences are listed in Table S1. Arrows 1 and 2 (left gel image) indicate representative TMD bands that are altered in the allohexaploid.

3. Methylation alterations in either S1 or S2, followed by an absence of TMD bands in subsequent generations, occurred for ~3% (13 bands, Table 1) of the TMD changes.
4. Appearance of novel unmethylated bands (bands present in both H and M lanes) in the amphiploid occurred for ~5% (25 bands, Table 1) of the TMD changes.
5. Appearance of novel methylated bands (present in either H or M lanes) in the amphiploid occurred for ~20% (98 bands, Table 1) of the TMD changes.

Figure 2B indicates that most of the band absence (~70%) occurred in the S1 generations and decreased dramatically in the subsequent generations, while no band absence was detected in S4 (Figure 2B). On the other hand, appearance of novel bands in the amphiploid occurred in ~57% of the cases in the S2 generation and were reduced in subsequent generations (Figure 2C).

A subset of 10 TMD bands was randomly chosen, extracted from the acrylamide gel, reamplified, and sequenced. Although all bands contained *Veju* LTR sequences at one end, their other ends contained LTR-flanking host DNA, two of which corresponded to wheat ESTs (accession nos. CD888659 and CJ569351) while the remainder were not found in wheat databases (see details in Table S5 and Table S6).

Validation of methylation changes by site-specific PCR: For validation of the methylation state, the 10 sequenced TMD bands mentioned above were further analyzed by site-specific PCR. While one band did not produce positive PCR products, the remaining 9 produced clear PCR products. To test the methylation status of CCGG sites in the *Veju* 5′ LTR by site-specific PCR, a primer was generated from the DNA sequence flanking the LTR (Figure 3, P4) of each one of the 10 sequences and used in PCR, in which undigested genomic DNA or DNA digested with either *Hpa*II or *Msp*I served as template. Specifically, the second primer was generated from a *Veju* 5′ LTR sequence upstream of the *Hpa*II and *Msp*I sites (five CCGG sites) (Figure 3, P6). The presence of a band in both the *Hpa*II and the *Msp*I lanes indicates that the LTR was methylated, the

TABLE 1

Classification of 486 TMD fragments that were altered in the amphiploid

Type of alteration	No. of bands	% from total altered bands
Methylation alteration	319	65.64
Absence of bands already in S1	31	6.38
Methylation alteration in S1 or S2 followed by absence of bands in subsequent generations	13	2.68
Appearance of novel unmethylated bands in S generations	25	5.14
Appearance of novel methylated bands in S generations	98	20.16
Total	486	100

results of a fragment not being digested. In all 9 cases, the results of the site-specific PCR validated the TMD results (Figure 3 and Figure S3). For example, the analysis of two TMD fragments, termed *Veju1* and *Veju2* (Figure 3, *Veju1* panel, and Figure 1, arrow 1), revealed that for *Veju1*, the insertion was unique to the TQ27 parental line and underwent demethylation (lack of PCR product in M lane, Figure 3) in the S1 generation. However, the band was absent in the subsequent generation as was seen also in TMD (Figure 1, arrow 1). For *Veju2*, the insertion was not seen in either the parental lines or the S1 generation; however, it was present in S2–S4 generations and was methylated (Figure 3, *Veju2* panel, and Figure 1, arrow 2). In all other cases (Figure S3), the results of site-specific PCR were in full agreement with the TMD results.

Correlation between cytosine methylation and *Veju* rearrangements in the newly formed allohexaploid: The TMD analysis (Table 1) indicated that ~35% of the changes in the amphiploid could be due to deletions or new insertions of *Veju* elements. In addition, the deletion (13 bands in Table 1) or possible new insertions (98 bands in Table 1) could indicate the possible correlation between methylation and rearrangements of *Veju*. To validate these claims, a TD was performed using a methylation-insensitive restriction enzyme, *Mse*I, together with a *Veju*-specific primer (see MATERIALS AND METHODS). Note that, in all cases where TMD bands disappeared in the S2 generation (Figure 2B), a methylation change (hypomethylation) occurred in the S1 generation. Similarly for newly appeared bands in the S2 generation (Figure 2C), the novel bands were accompanied by methylation.

Figure 4 confirms that indeed deletion of *Veju*-containing sequences occurs already in the S1 generation (for example, bands 1 and 2, Figure 4), or it can occur in S2 (for example, bands 3–5, Figure 4). It is important to note that the ~9% of the TMD changes that could be related to deletion of *Veju*-containing sequences (Table 1) could be underestimated because deletion of bands can be seen only among the polymorphic bands (in the TMD or TD gels) in the two parental lines. In addition, the TD analysis confirms the insertions of *Veju* sequences in the S2 generation (for example, bands 6–12, Figure 4). Extraction of four newly inserted bands and five deleted bands in the S2 generation from the TD gel, reamplification, and sequencing indicated that two newly inserted sequences and three deleted bands were already detected in the previous TMD experiments, whereas the newly inserted sequences in the S2 generation were methylated, and all three deleted bands in S2 were hypomethylated in S1. These data—together with the fact that all deleted bands in the S2 generation had changed their methylation pattern in S1 (hypomethylated), and all newly inserted bands in S2 were accompanied with methylation—indicate the direct link between methyl-

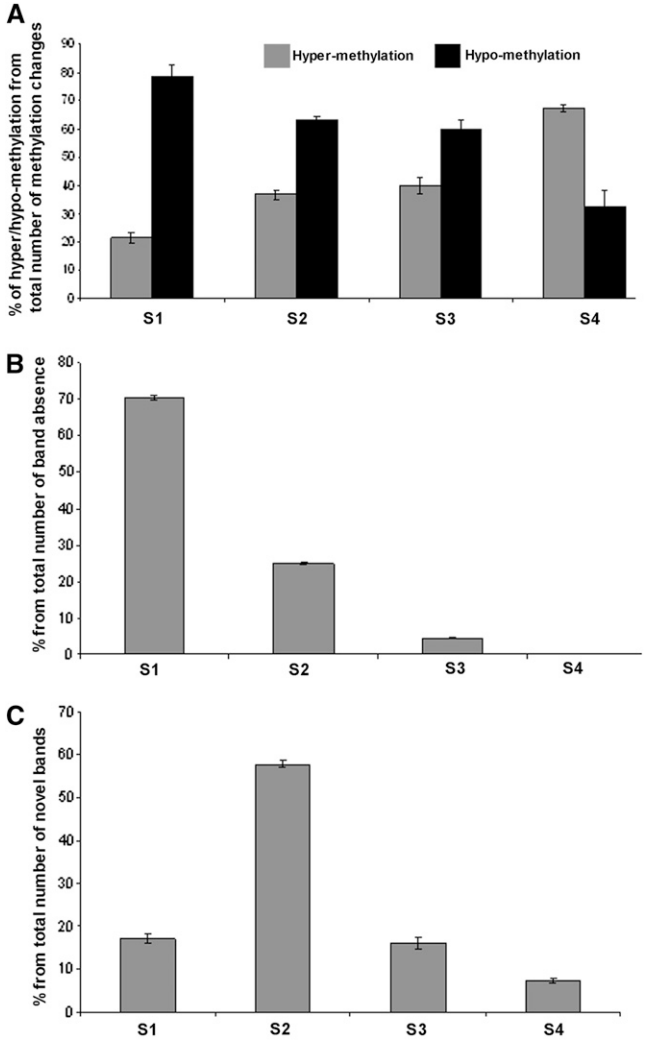

FIGURE 2.—Analysis of changes in TMD patterns among the first four generations (S1–S4) of the newly formed allohexaploid. (A) Level of hypomethylation *vs.* hypermethylation from the total number of methylation changes in each generation. (B) Level of absence of TMD bands in each generation. (C) Level of appearance of novel bands (that were not seen in the parental lines) in each generation.

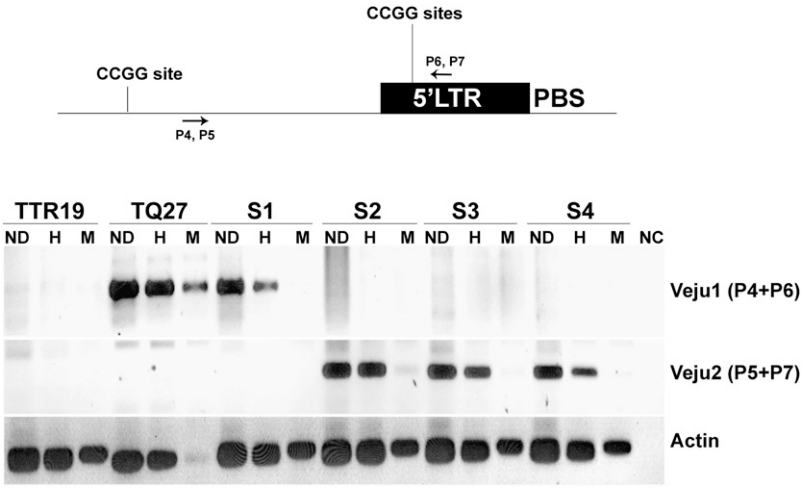

FIGURE 3.—Methylation of CCGG sites in the LTR. (Top) An LTR and flanking sequences shown together with the cleavage sites (CCGG) of the restriction enzymes *Hpa*II and *Msp*I (five CCGG sites upstream of P6 and P7 in the LTR) and the position of primers used in PCR analysis. (Bottom) PCR analysis (using primer pairs P4 and P6 for *Veju1* or P5 and P7 for *Veju2*) of LTR methylation in leaves using undigested genomic DNA (ND) or DNA digested with either *Hpa*II (H) or *Msp*I (M) as the template (from parental lines and the first four generations of the derived allohexaploid). Primer sequences are listed in Table S1. Actin was used as a control for DNA quality, while no CCGG sites are present in the amplified region. As a negative control, water was used as template in the PCR reaction.

ation and rearrangements of *Veju* in the newly formed allohexaploid. Note that the flanking sequences of all nine chimeric isolated TD bands did not hit any known sequence in the database, except one newly inserted sequence that significantly hit a telomeric region (*Hordeum vulgare* telomeric chromosome 7H region).

Additional support for the link between methylation and *Veju* rearrangements came from the site-specific PCR analysis (Figure 3, *Veju1* and *Veju2* panels, and Figure S3a). For *Veju1* (Figure 3), it can be seen clearly that the demethylation of the element in the S1 generation was followed by its deletion in subsequent generations, while, for *Veju2*, a new insertion occurred in the second generations of the newly formed allohexaploid (Figure 3) that was accompanied by methylation of the new insertion. In another case (Figure S3a), a partially methylated *Veju* insertion in TTR19 parental lines was deleted in the S2 generation. Further validations of the deleted *Veju1* and the newly inserted *Veju2* were performed (see details in Figure S4 and Figure S5). Finally, the methylation of the new insertion (*Veju 2*) was further validated by bisulfite sequencing (Figure S6).

Precise developmental timing of *Veju1* deletion and *Veju*2 insertion: The developmental timing of the deletion or insertion of *Veju* sequences was tested by isolating DNA from (1) the pollen grains, ovaries, and first true leaves of S1 plants and (2) the immature seeds (*i.e.*, 2 weeks after fertilization), mature embryos, first roots, and first leaves of S2 plants. The isolated DNA served as a template for PCR. For *Veju1* (the deleted element in the S2 generation), PCR was performed using primers P8 and P10 (see Figure S5), designed to amplify a 193-bp fragment of the host flanking sequence. The band was detected in all S1 tissues but was absent from S2 tissues (Figure 5A, top), indicating that it was eliminated during the early stages of S2 embryo development. Similarly, PCR amplification of *Veju2* (new insertion in S2 generation) was performed using primers P5 and P7 (see Figure 3) to amplify a 304-bp chimeric (*Veju*/host flanking) sequence. The band was absent in all S1 tissues yet present in S2 tissues (Figure 5A, bottom), indicating that *Veju2* insertion occurred during the early stages of S2 embryo development. To validate these results, TD was performed in S2 embryos (Figure 5B),

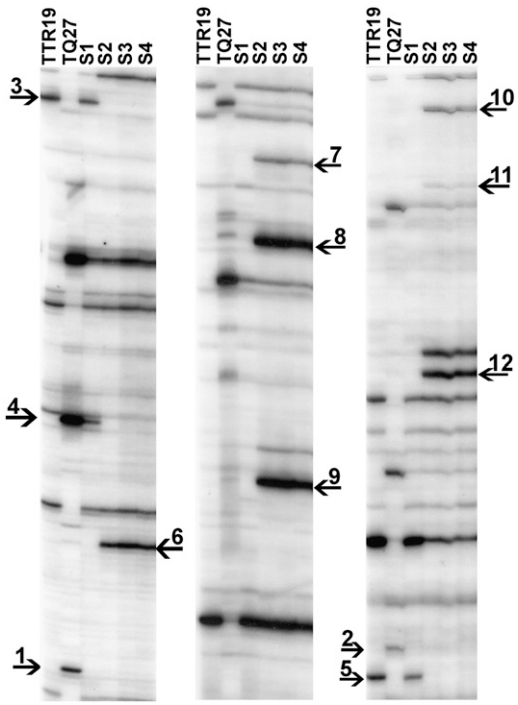

FIGURE 4.—*Veju* deletion and insertion as displayed by TD patterns in *T. turgidum* ssp. *durum* (TTR19) and *Ae. tauschii* (TQ27) and in the first four generations (S1–S4) of the derived allohexaploid. *Mse*I, methylation-insensitive enzyme, was used for DNA cleavage. Autoradiographs of TD used P2 and the *Mse*I-adapter primer. (Left) +(CAC). (Middle) +(CTG). (Right) +(CAT). Primer sequences are listed in Table S1. Arrows indicate deleted or newly inserted *Veju* elements in the newly formed allohexaploid (see text).

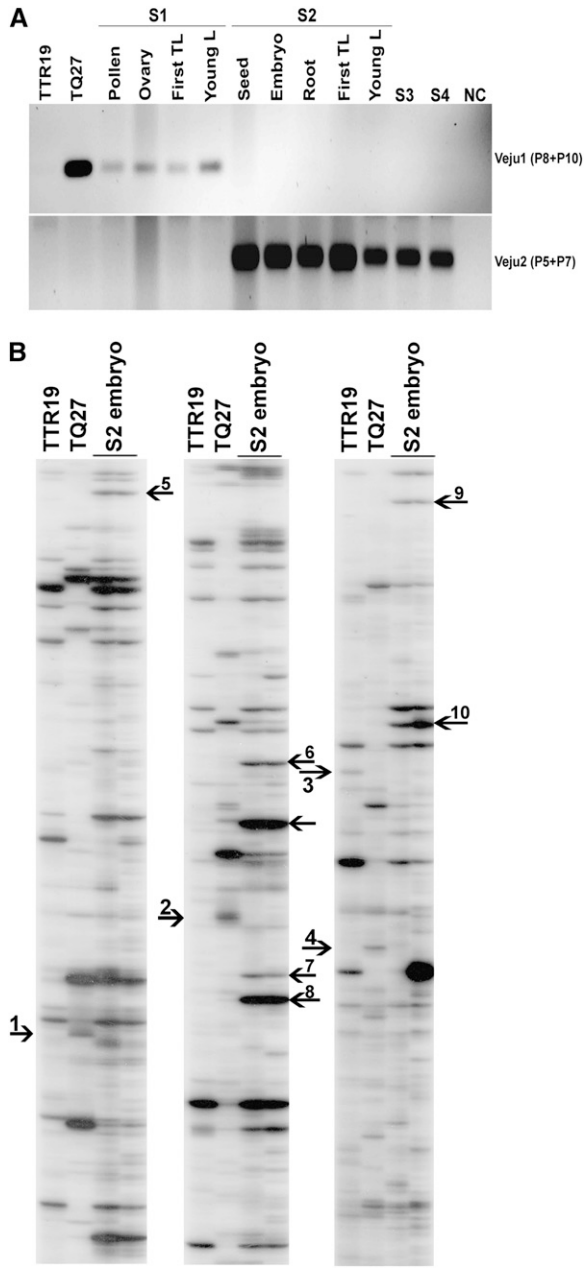

FIGURE 5.—Developmental timing of deletion of *Veju*-containing fragments and new *Veju* insertions. (A) PCR analysis using primers P8 + P10 for *Veju1* (top), and P5 + P7 for *Veju2* (bottom) (see primer positions in Figure 3) on DNA templates of parental lines (TTR19 and TQ27); pollen, ovary, first true leaf (First TL), and young leaf of S1; seed, embryo, first roots, first true leaf, and young leaf of S2; S3; and S4. As negative control, water served as a template in a PCR reaction. (B) *Veju* deletion and insertion as displayed by TD patterns in *T. turgidum* ssp. *durum* (TTR19) and *Ae. tauschii* (TQ27) and in the S2 embryo. Primes used in TD reaction are the same as used in Figure 4. Arrows indicate deleted or newly inserted *Veju* elements in the embryos of the S2 generation (see text).

and it is clearly seen that deletion (for example, bands 1–3, Figure 5B) or insertion (for example, bands 4–10, Figure 5B) of *Veju* occurred in the embryo. These data

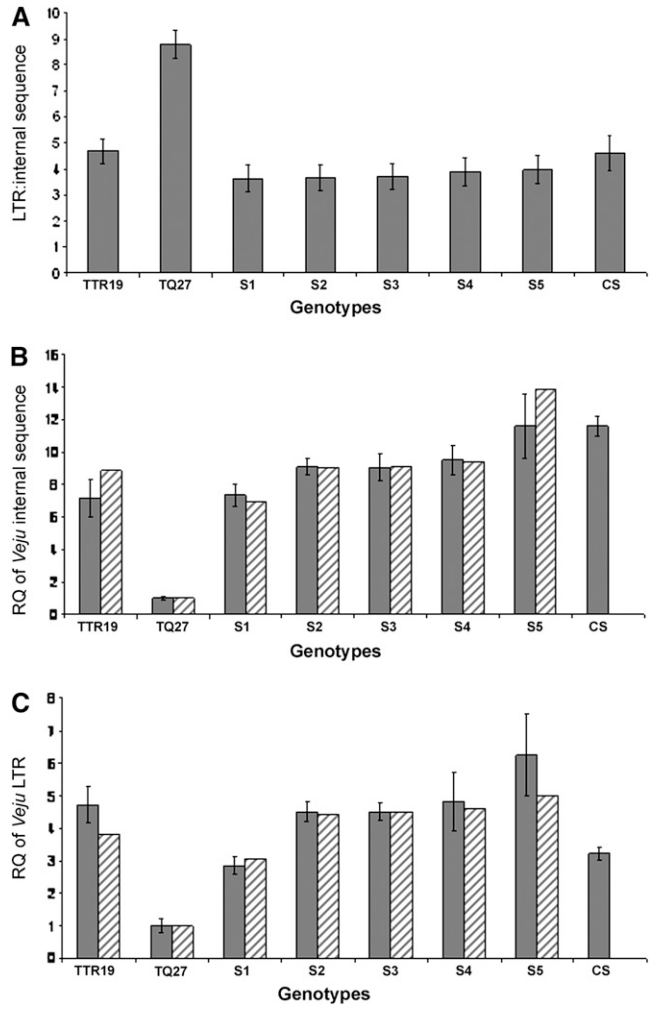

FIGURE 6.—Quantitative PCR analysis of *Veju* retrotransposons in parental lines and in the S1–S5 generations of the derived allohexaploid. In addition, the natural hexaploid *T. aestivum* (cv. *Chinese spring*–CS) was used for comparison. (A) LTR:internal *Veju* sequence. (B) Relative quantity (RQ) of the *Veju* internal region (sequence). (C) RQ of the *Veju* LTR. Shaded bars represent the observed relative quantity (mean ± SE, $n = 3$), while hatched bars represent the expected relative quantity (see text for qPCR validation).

indicate that rearrangement of *Veju* may occur somatically, transpiring as early as during zygote formation.

Quantitative evaluation of *Veju* composition in the newly formed allohexaploid and its parental lines: Our observation that the TMD patterns of *Veju* insertion sites changed dramatically (~55%) in the newly formed allohexaploid, relative to its progenitors, and the fact that *Veju* methylation status can be correlated with *Veju* deletion and/or insertion facilitated the design of experiments to quantitatively test *Veju* composition using real-time PCR. Specifically, qPCR was used to calculate the ratio of *Veju* LTRs to *Veju* internal sequences to estimate the proportions of solo LTRs and intact elements. DNA serving as qPCR template was isolated from the parental lines and the S1 and S5 generations. Two primer pairs, one specific to the LTR sequence and

the other designed from internal *Veju* sequences (Table S2), were employed. Figure 6A shows the relative quantities of *Veju* internal sequences and LTRs in the genomes of the parental lines, TTR19 and TQ27, and in those of the S1–S5 generations. The average internal sequence:LTR ratios were 1:4.7 in TTR19, 1:8.8 in TQ27, 1:3.7 in S1, 1:3.6 in S2, 1:37 in S3, 1:3:9 in S4, and 1:4 in S5. Most importantly, while the S1–S5 generations of the newly formed allohexaploid are each expected to possess an intermediate internal sequence:LTR ratio (~1:6.75), relative to those of the two parental lines, in fact the offspring generations exhibited reductions of ~43%, indicating that a massive number of LTRs may have been deleted in the newly formed allohexaploid. Interestingly, qPCR analysis of the newly formed allohexaploid displayed similar results as achieved with the natural hexaploid *Triticum aestivum* (cv. *Chinese spring*) (Figure 6A).

The observation that the number of *Veju* LTRs was significantly reduced in allohexaploid generations led to the design of experiments to test for changes in *Veju* element copy numbers in the newly formed allohexaploid. Relative *Veju* element quantities were measured in the parental lines and in the S1 and S5 generations using the single-copy vernalization gene 1 (*VRN1*) as a reference. Three orthologs of *VRN1* that distinguish the AA, BB, and DD genomes of hexaploid wheat are correspondingly located in chromosomes 5A (Law *et al.* 1976; Dubcovsky *et al.* 1998), 5B (Barrett *et al.* 2002; Iwaki *et al.* 2002), and 5D (Law *et al.* 1976). Therefore, *VRN1* exists in one copy in a diploid progenitor, in two copies in a tetraploid progenitor, and in three copies in the newly formed allohexaploid. To this end, a PCR reaction was performed as previously described ((Yan *et al.* 2004) to amplify the three *VRN1* orthologs in the parental lines and in the S1 and S5 generations to ensure that *VRN1* was not affected by the allopolyploidization process (Figure S7).

For the qPCR experiments, primers to *VRN1* were designed on the basis of the multiple sequence alignment of previously published sequences from a conserved region of exon 4 (Figure S8). Our use of exon 4 enabled us to avoid amplifying a conserved MADS box encoded by the first exons (Yan *et al.* 2003) (Table S2 and Figure S8). Relative quantities of *Veju* internal sequences in the parental lines and in the S1–S5 genomes were measured using qPCR with primers specific for the *Veju* internal sequence (Figure 6B, shaded bars) (see Table S2). The copy number of *Veju* elements in the newly formed allohexaploid is expected to be the sum of the copy numbers of the two parental lines. While S1 displayed a reduction of ~9.8% from this expected value, the subsequent generations displayed a >40% increase in *Veju* copy number relative to S1 (Figure 6B, shaded bars). These results indicate that a loss of *Veju* sequences in the first generation of the newly formed allohexaploid was followed by an accumulation of new *Veju* insertions in subsequent generations. Indeed, the copy number of *Veju* in the S5 generation was similar to the copy number of this sequence in the natural hexaploid (Figure 6B). Note that deletion of *Veju*-containing sequences might be completed in S4 (see Figure 2B), while *Veju* elements remain active (see Figure 2C), which may explain the relatively high quantities displayed in S5, even though the increase in S5 is not statistically significant compared to S4.

Relative *Veju* LTR quantities were also measured in the parental lines and in the S1 and S5 generations using LTR-specific primers (Figure 6C, shaded bars). As predicted from the previous experiment (Figure 6A), the S1 generation showed a reduction in LTR content of ~50% from the number of *Veju* LTR copy numbers expected. The estimated quantity of *Veju* LTRs in S2–S5 indicated that these sequences were markedly reduced in the S1 generation and that a burst of insertions accrued in subsequent generations. However, as the *Veju* LTR content in the natural hexaploid was similar to that of S1, this might indicate that throughout evolution LTRs (or solo LTRs) are continuously removed from the genome.

All qPCR experiments had three biological replicates (see materials and methods, *Quantitative PCR*). Quality control for qPCR experiments to rule out possible competition effects in the PCR reactions using template mix was also performed (Figure S9). In addition, LTR:*Veju* internal sequence ratios were used to validate the observed relative quantities of *Veju* internal sequences and LTRs in the parental lines and in the S1 and S5 generations. Assuming that the observed ratios between the *Veju* elements are correct (Figure 6A), then the expected relative quantities of *Veju* LTRs (Figure 6C, hatched bars) should be calculable on the basis of the observed relative quantities of *Veju* internal sequences (Figure 6B, shaded bars). This can be realized by multiplying the observed relative quantities of *Veju* internal sequences by the observed LTR:internal sequence ratio (*i.e.*, 4.7 in TTR19, 8.8 in TQ27, 3.7 in S1, and 3.4 in S5). For example, the expected relative quantity of *Veju* LTRs in the S1 generation will be the observed relative quantity of *Veju* internal sequence (Figure 6B, shaded bars) multiplied by 3.7. Similar calculations were also used to determine the expected relative quantities of *Veju* internal sequences, but in this case, the observed relative LTR quantities (Figure 6C, shaded bars) were divided, not multiplied, by the LTR:internal *Veju* sequence ratios. For example, the expected relative quantity of *Veju* internal sequences (Figure 6B, hatched bars) in the S1 generation can be attained by taking the observed relative quantity of *Veju* LTRs (Figure 6C, shaded bars) and dividing by 3.7. After such calculations, nearly complete agreement between the expected and the observed relative quantities was achieved for both *Veju* LTR and internal sequence experiments.

DISCUSSION

This study pinpointed changes in the methylation patterns of >880 *Veju* insertion sites using TMD. We found that ~54% of the TMD patterns were altered in the first four generations of a newly formed allohexaploid. Using TMD and TD, we have observed deletions and/or new insertions of *Veju* elements in the newly formed allohexaploid, and in many cases we found that these alterations were correlated with changes in cytosine methylation. These observations led us to address the genomic compositions of *Veju* elements in S1–S5 generations of the newly formed allohexaploid. Surprisingly, we found that *Veju* elements, especially *Veju* LTRs, underwent massive deletions in the S1 generation and moderate insertions in subsequent generations. In addition, we noted that *Veju* rearrangements seemed to occur immediately after meiosis and formation of the zygote. This developmental timing might have important consequences as other work showed that TEs are epigenetically silenced in gametes, while they are active in the pollen vegetative nucleus (Slotkin *et al.* 2009).

Methylation of *Veju* elements: On the basis of TMD analysis, we estimated that ~41% of the CCGG sites flanking *Veju* elements could be cytosine-methylated in the young leaves of the parental lines *T. turgidum* ssp. *durum* (TTR19) and *Ae. tauschii* (TQ27). Over 54% of the *Veju* insertion sites in the parental plants showed altered TMD patterns in the first four generations (S1–S4) of the newly formed allohexaploid. In most cases, *Veju* sites were hypomethylated in the first generation (S1) of the newly formed allohexaploid, while hypermethylation was predominant in the S4 generation (Figure 2A). It is important to note that the analysis was performed qualitatively by assessing polymorphic *vs.* monomorphic bands. Furthermore, it is known that DNA methylation can vary from cell to cell in the same tissue, an outcome that can lead to different band intensities in a TMD gel.

The observed methylation and changes in TMD patterns of *Veju* insertion sites were significantly higher than one would expect from random methylation. Indeed, whole-genome methylation changes reported in newly formed allotetraploids are typically ~13% (Shaked *et al.* 2001). Results similar to ours were reported for Spartina species, in which higher-than-random methylation was observed for the flanking sequences of three studied TEs (Parisod *et al.* 2009).

Our TMD analysis revealed that, in ~23% of cases (Table 1), methylation alteration was accompanied by a deletion and/or insertion of *Veju* sequences. Most of the bands that were deleted in the newly formed allohexaploids were from the DD genome of TQ27, which could indicate that *Veju* loci inherited from the TQ27 parent in the newly formed allohexaploids may be more vigorously targeted for methylation/elimination than those inherited from the TTR19 parent. Accordingly, parent-dependent changes in TE methylation patterns were also reported in Spartina hybrids, in which the majority of the altered bands after hybridization, predominantly band losses, were of maternal origin (Parisod *et al.* 2009). However, in our case, TQ27 is the paternal line, so the phenomenon is more likely correlated with genome composition rather than with paternal origin (imprinting) because the same results were observed in reciprocal crosses. For example, Ozkan *et al.* (2001) and Shaked *et al.* (2001) reported the same pattern of DNA sequence elimination in reciprocal crosses of newly synthesized allopolyploids.

Our data indicate that deletion of *Veju*-containing sequences occurred in the S1–S3 generations of the amphiploid, while no deletion events were detected in the S4 (Figure 2B). This is in agreement with what was previously reported by Ozkan *et al.* (2001), who proposed that deletion of low-copy sequences in newly formed wheat allopolyploids was completed in the S3 generation.

TMD, TD analysis, and site-specific PCR experiments clearly indicated that a change in the methylation status (usually hypomethylation) in the S1 generation was followed by deletion in the S2 generation (Figures 1 and 3 and Figure S3). In addition, newly inserted *Veju* elements in the S2 generation exhibited LTR methylation. These data clearly show the correlation between methylation and post-allopolyploidization rearrangements that occur via a yet to be identified mechanism. In addition, small RNA corresponding to *Veju* elements might play a prominent role in *Veju* methylation in the newly formed allohexaploid (Avi Levy, personal communication).

Quantitative analysis of *Veju* by qPCR: The existence of solo LTRs for nonautonomous elements and their evolutionary roles have been described for TRIM and LARD elements (Witte *et al.* 2001; Kalendar *et al.* 2004). However, detailed information about the extent and the timing of their formation in newly formed allopolyploids has yet to be studied. In this study, we performed a quantitative evaluation of the genomic composition of *Veju* elements using qPCR analysis.

The ratio of intact elements to solo LTRs fluctuates greatly between retrotransposons in different plant species—from ~8:1 (eight intact elements to one solo LTR) in soybean (Wawrzynski *et al.* 2008), implying very slow rates of TE sequence removal, to ~1:9 (one intact element to nine solo LTRs) for LARD retrotransposons in barley, probably due to abundant homologous recombination events (Kalendar *et al.* 2004). Our estimation of the genomic distribution of *Veju* elements showed that the genomes of the parental lines TTR19 and TQ27 possessed as many as 2.7 to 6.8 times more LTRs, respectively, than intact *Veju* elements.

The inherited *Veju* sequences exhibited clear losses of parental additivity. We observed an ~44% reduction from the expected LTR:internal *Veju* ratios in newly

formed allohexaploids, a finding that infers new genome reorganization following allopolyploidization and a massive loss of *Veju* LTRs. Moreover, we report a dramatic reduction in the relative quantities of *Veju* LTRs (~40%) in the S1 generation (Figure 6, A and C). Apparently, the newly formed allopolyploid genome has attempted to reduce its burden of genetic "junk." It is important to note that the qPCR data (Figure 6) and the TMD data (Figures 1 and 2) were in very good agreement, both indicating that most deletions of *Veju* sequences occurred in the S1 while most new insertions occurred in the S2 generation.

Species- and parent-specific elimination of high-copy genomic sequences has recently been reported in other plant allopolyploids. It was documented in Triticale (a synthetic allopolyploid hybrid produced by crossing wheat and rye) that allopolyploidy is associated with extensive, genome-wide genomic rearrangement. Prominent among these changes is the elimination of rye-specific fragments that often represent retrotransposons or their derivatives (Bento *et al.* 2008). In newly formed tobacco allopolyploids, parent-specific elimination of DNA repeats to a degree as high as 60% was also documented (Skalicka *et al.* 2005). In light of our observation that ~68% of the TMD bands unaccounted for in the allopolyploids were from the DD genome, we propose that most TE elimination originated from the ancient DD genome while targeting solo LTRs or truncated elements for elimination.

Intriguingly, an increase in both *Veju* LTRs and internal regions was observed in the S5 generation. Considered together with the observed transcriptional activity of *Veju*, these results indicate that the immense loss of *Veju* sequences in the first generation after genome doubling is probably followed by retrotransposition in subsequent generations, a process that causes new insertions to accumulate in allohexaploids. Although some restructuring in the vicinity of TEs was reported in natural, 150-year-old *Spartina anglica* allopolyploids, no TE transposition was detected (Parisod *et al.* 2009). TE activation in newly formed allopolyploids, therefore, may be species-specific and limited to certain TEs.

A comparison of the genomic distribution of *Veju* in the S5 generation and in the ~10,000-year-old natural hexaploid (Figure 6) revealed similar LTR:internal sequence ratios and similar quantities of *Veju* internal sequences. This might indicate that most rearrangements occur in the earliest generations of the nascent allopolyploid rather than on an evolutionary scale. This explains the data from Charles *et al.* (2008), according to which allopolyploidization neither enhanced nor repressed retrotranspositions when tested on an evolutionary timescale.

In natural populations, the abrupt proliferation of TEs could have important biological significance (Belyayev *et al.* 2009). First, differential TE insertion into the chromosomes of different parental genomes would reduce homologous recombination and promote disomic inheritance, thereby stabilizing the newly formed genome and increasing the fertility of the nascent allopolyploid species. Second, differential TE insertion contributes to genetic diversity and induces polymorphism in newly formed allopolyploids, a process that may increase allopolyploid fitness in different environments.

Underlying mechanisms for *Veju* elimination: In plants, most of the full-length retrotransposons were estimated to be <5 million years old (Sanmiguel *et al.* 2002; Vitte and Panaud 2003; Wicker *et al.* 2003; Ma *et al.* 2004; Du *et al.* 2006; Wicker and Keller 2007; Charles *et al.* 2008), indicating that active deletion mechanisms that remove LTR retrotransposons from the genome exist. One molecular mechanism that may be responsible for massive LTR and internal *Veju* sequence loss in the first generation is unequal intrastrand homologous recombination. In rice, solo LTRs probably originated from intra-element recombination events (Vitte and Panaud 2003). In wheat allopolyploids, however, it is more likely that the observed rearrangements resulted from interelement recombination, which can affect more transposons than intra-element recombination and which can also eliminate flanking *Veju* sequences. In addition to unequal homologous recombination, illegitimate recombination is also a key process for retrotransposon deletion in rice (Ma *et al.* 2004). Moreover, illegitimate recombination was found to be the main cause of LTR-retrotransposon removal in *Arabidopsis thaliana* (Devos *et al.* 2002; Bennetzen *et al.* 2005) and the cause of LTR retroelement deletions in diploid and polyploid wheat and allopolyploid cotton. Thus, increased illegitimate recombination may be a general consequence of polyploidization (Wicker *et al.* 2003; Chantret *et al.* 2005; Grover *et al.* 2007).

Thus far, we do not have clear, definitive support for any of the mechanisms suggested as the driving force behind the observed high rates of genomic change between generations of allohexaploid wheat species. On the one hand, the finding that LTR levels were high in the parental lines, relative to the levels of intact elements, suggests that unequal homologous recombination is the more active and, therefore, more likely mechanism behind TE deletions (Ma *et al.* 2004). On the other hand, while unequal homologous recombination requires large (>50 bp) stretches of sequence homology, illegitimate recombination requires only a few base pairs of sequence identity, suggesting that illegitimate recombination is more widely applicable than unequal homologous recombination and, as such, is responsible for more deletions, including those of *Veju*-flanking sequences, than is unequal homologous recombination. Strikingly, a long form of the *Veju* retrotransposon was proposed to have originated from an

illegitimate heterologous recombination (Sabot *et al.* 2005b), suggesting that this element can act as a "hot spot" that attracts illegitimate rearrangements. The molecular mechanism by which hypomethylated *Veju* elements undergo deletion remains unknown. Perhaps hypomethylation of *Veju* elements indicates an open chromatin that exposes these demethylated elements as targets for deletion by the host. As mentioned above, small RNAs might also have a major role in this process. On the other hand, methylation of new *Veju* insertions can be understood as a defensive mechanism of the host from the deleterious transposon insertions. Nevertheless, future studies should address these processes and their biological significance in nascent allopolyploids.

We thank Hakan Ozkan and Moshe Feldman for providing the amphiploid material and Avi Levy for helpful discussions. This work was supported by a grant from the Israel Science Foundation (grant no. 142/08) to K.K.

LITERATURE CITED

Adams, K. L., and J. F. Wendel, 2004 Exploring the genomic mysteries of polyploidy in cotton. Biol. J. Linn. Soc. **82:** 573–581.

Adams, K. L., and J. F. Wendel, 2005a Novel patterns of gene expression in polyploid plants. Trends Genet. **21:** 539–543.

Adams, K. L., and J. F. Wendel, 2005b Polyploidy and genome evolution in plants. Curr. Opin. Plant Biol. **8:** 135–141.

Adams, K. L., R. Cronn, R. Percifield and J. F. Wendel, 2003 Genes duplicated by polyploidy show unequal contributions to the transcriptome and organ-specific reciprocal silencing. Proc. Natl. Acad. Sci. USA **100:** 4649–4654.

Ainouche, M. L., P. M. Fortune, A. Salmon, C. Parisod, M. A. Grandbastien *et al.*, 2009 Hybridization, polyploidy and invasion: lessons from Spartina (Poaceae). Biol. Invasions **11:** 1159–1173.

Barrett, B., M. Bayram and K. Kidwell, 2002 Identifying AFLP and microsatellite markers for vernalization response gene Vrn-B1 in hexaploid wheat using reciprocal mapping populations. Plant Breed. **121:** 400–406.

Beaulieu, J., M. Jean and F. Belzile, 2009 The allotetraploid *Arabidopsis thaliana-Arabidopsis lyrata* subsp *petraea* as an alternative model system for the study of polyploidy in plants. Mol. Genet. Genomics **281:** 421–435.

Belyayev, A., R. Kalendar, L. Brodsky, E. Nevo, A. H. Schulman *et al.*, 2009 Transposable elements in a marginal plant population: temporal fluctuations provide new insights into genome evolution of wild diploid wheat. Mobile DNA **1:** 1–16.

Bennetzen, J. L., and E. A. Kellogg, 1997 Do plants have a one-way ticket to genomic obesity? Plant Cell **9:** 1509–1514.

Bennetzen, J. L., J. X. Ma and K. Devos, 2005 Mechanisms of recent genome size variation in flowering plants. Ann. Bot. **95:** 127–132.

Bento, M., H. S. Pereira, M. Rocheta, P. Gustafson, W. Viegas *et al.*, 2008 Polyploidization as a retraction force in plant genome evolution: sequence rearrangements in *Triticale*. PLoS One **3:** 1402–1413.

Capy, P., G. Gasperi, C. Biemont and C. Bazin, 2000 Stress and transposable elements: Co-evolution or useful parasites? Heredity **85:** 101–106.

Chantret, N., J. Salse, F. Sabot, S. Rahman, A. Bellec *et al.*, 2005 Molecular basis of evolutionary events that shaped the hardness locus in diploid and polyploid wheat species (Triticum and Aegilops). Plant Cell **17:** 1033–1045.

Charles, M., H. Belcram, J. Just, C. Huneau, A. Viollet *et al.*, 2008 Dynamics and differential proliferation of transposable elements during the evolution of the B and A genomes of wheat. Genetics **180:** 1071–1086.

Chen, Z. J., 2007 Genetic and epigenetic mechanisms for gene expression and phenotypic variation in plant polyploids. Annu. Rev. Plant Biol. **58:** 377–406.

Chen, Z. J., and Z. F. Ni, 2006 Mechanisms of genomic rearrangements and gene expression changes in plant polyploids. BioEssays **28:** 240–252.

Chen, Z. J., and C. S. Pikaard, 1997 Transcriptional analysis of nucleolar dominance in polyploid plants: biased expression/silencing of progenitor rRNA genes is developmentally regulated in Brassica. Proc. Natl. Acad. Sci. USA **94:** 3442–3447.

Comai, L., A. P. Tyagi, K. Winter, R. Holmes-Davis, S. H. Reynolds *et al.*, 2000 Phenotypic instability and rapid gene silencing in newly formed *Arabidopsis* allotetraploids. Plant Cell **12:** 1551–1567.

Devos, K. M., J. K. M. Brown and J. L. Bennetzen, 2002 Genome size reduction through illegitimate recombination counteracts genome expansion in Arabidopsis. Genome Res. **12:** 1075–1079.

Du, C. G., Z. Swigonova and J. Messing, 2006 Retrotranspositions in orthologous regions of closely related grass species. BMC Evol. Biol. **6:** 62.

Dubcovsky, J., D. Lijavetzky, L. Appendino and G. Tranquilli, 1998 Comparative RFLP mapping of *Triticum monococcum* genes controlling vernalization requirement. Theor. Appl. Genet. **97:** 968–975.

Feschotte, C., N. Jiang and S. R. Wessler, 2002 Plant transposable elements: where genetics meets genomics. Nat. Rev. Genet. **3:** 329–341.

Grandbastien, M., C. Audeon, E. Bonnivard, J. M. Casacuberta, B. Chalhoub *et al.*, 2005 Stress activation and genomic impact of Tnt1 retrotransposons in Solanaceae. Cytogenet. Genome Res. **110:** 229–241.

Grover, C. E., H. Kim, R. A. Wing, A. H. Paterson and J. F. Wendel, 2007 Microcolinearity and genome evolution in the AdhA region of diploid and polyploid cotton (Gossypium). Plant J. **50:** 995–1006.

Iwaki, K., J. Nishida, T. Yanagisawa, H. Yoshida and K. Kato, 2002 Genetic analysis of Vrn-B1 for vernalization requirement by using linked dCAPS markers in bread wheat (Triticum aestivum L.). Theor. Appl. Genet. **104:** 571–576.

Kalendar, R., C. M. Vicient, O. Peleg, K. Anamthawat-Jonsson, A. Bolshoy *et al.*, 2004 Large retrotransposon derivatives: abundant, conserved but nonautonomous retroelements of barley and related genomes. Genetics **166:** 1437–1450.

Kashkush, K., and V. Khasdan, 2007 Large-scale survey of cytosine methylation of retrotransposons and the impact of readout transcription from long terminal repeats on expression of adjacent rice genes. Genetics **177:** 1975–1985.

Kashkush, K., M. Feldman and A. A. Levy, 2002 Gene loss, silencing and activation in a newly synthesized wheat allotetraploid. Genetics **160:** 1651–1659.

Kashkush, K., M. Feldman and A. A. Levy, 2003 Transcriptional activation of retrotransposons alters the expression of adjacent genes in wheat. Nat. Genet. **33:** 102–106.

Kidwell, K. K., and T. C. Osborn, 1992 Simple plant DNA isolation procedures, pp. 1–13 in *Plant Genomes: Methods for Genetic and Physical Mapping*, edited by J. S. Beckmann and T. C. Osborn. Kluwer Academic Publishers. Dordrecht, The Netherlands.

Law, C. N., A. J. Worland and B. Giorgi, 1976 Genetic control of ear emergence time by chromosomes 5a and chromosomes 5d of wheat. Heredity **36:** 49–58.

Levy, A. A., and M. Feldman, 2002 The impact of polyploidy on grass genome evolution. Plant Physiol. **130:** 1587–1593.

Liu, B., J. M. Vega and M. Feldman, 1998a Rapid genomic changes in newly synthesized amphiploids of *Triticum* and *Aegilops*. II. Changes in low-copy coding DNA sequences. Genome **41:** 535–542.

Liu, B., J. M. Vega, G. Segal, S. Abbo, H. Rodova *et al.*, 1998b Rapid genomic changes in newly synthesized amphiploids of *Triticum* and *Aegilops*. I. Changes in low-copy noncoding DNA sequences. Genome **41:** 272–277.

Livak, K. J., and T. D. Schmittgen, 2001 Analysis of relative gene expression data using real-time quantitative PCR and the 2(T) (-Delta Delta C) method. Methods **25:** 402–408.

Ma, J. X., K. M. Devos and J. L. Bennetzen, 2004 Analyses of LTR-retrotransposon structures reveal recent and rapid genomic DNA loss in rice. Genome Res. **14:** 860–869.

Madlung, A., R. W. Masuelli, B. Watson, S. H. Reynolds, J. Davison *et al.*, 2002 Remodeling of DNA methylation and phenotypic and transcriptional changes in synthetic *Arabidopsis* allotetraploids. Plant Physiol. **129:** 733–746.

Madlung, A., A. P. Tyagi, B. Watson, H. M. Jiang, T. Kagochi *et al.*, 2005 Genomic changes in synthetic *Arabidopsis* polyploids. Plant J. **41:** 221–230.

Matzke, M. A., and A. J. M. Matzke, 1998 Polyploidy and transposons. Trends Ecol. Evol. **13:** 241–241.

McClintock, B., 1984 The significance of responses of the genome to challenge. Science **226:** 792–801.

O'Neill, R. J. W., M. J. O'Neill and J. A. M. Graves, 1998 Undermethylation associated with retroelement activation and chromosome remodelling in an interspecific mammalian hybrid. Nature **393:** 68–72.

Osborn, T. C., J. C. Pires, J. A. Birchler, D. L. Auger, Z. J. Chen *et al.*, 2003 Understanding mechanisms of novel gene expression in polyploids. Trends Genet. **19:** 141–147.

Ozkan, H., A. A. Levy and M. Feldman, 2001 Allopolyploidy-induced rapid genome evolution in the wheat (*Aegilops-Triticum*) group. Plant Cell **13:** 1735–1747.

Parisod, C., A. Salmon, T. Zerjal, M. Tenaillon, M. A. Grandbastien *et al.*, 2009 Rapid structural and epigenetic reorganization near transposable elements in hybrid and allopolyploid genomes in Spartina. New Phytol. **184:** 1003–1015.

Rapp, R. A., and J. F. Wendel, 2005 Epigenetics and plant evolution. New Phytol. **168:** 81–91.

Sabot, F., R. Guyot, T. Wicker, N. Chantret, B. Laubin *et al.*, 2005a Updating of transposable element annotations from large wheat genomic sequences reveals diverse activities and gene associations. Mol. Genet. Gen. **274:** 119–130.

Sabot, F., P. Sourdille and M. Bernard, 2005b Advent of a new retrotransposon structure: the long form of the Veju elements. Genetica **125:** 325–332.

Salmon, A., M. L. Ainouche and J. F. Wendel, 2005 Genetic and epigenetic consequences of recent hybridization and polyploidy in *Spartina* (*Poaceae*). Mol. Ecol. **14:** 1163–1175.

SanMiguel, P. J., W. Ramakrishna, J. L. Bennetzen, C. S. Busso and J. Dubcovsky, 2002 Transposable elements, genes and recombination in a 215-kb contig from wheat chromosome 5A m. Funct. Integr. Genomics **2:** 70–80.

Shaked, H., K. Kashkush, H. Ozkan, M. Feldman and A. A. Levy, 2001 Sequence elimination and cytosine methylation are rapid and reproducible responses of the genome to wide hybridization and allopolyploidy in wheat. Plant Cell **13:** 1749–1759.

Simons, K. J., J. P. Fellers, H. N. Trick, Z. C. Zhang, Y. S. Tai *et al.*, 2006 Molecular characterization of the major wheat domestication gene Q. Genetics **172:** 547–555.

Skalicka, K., K. Y. Lim, R. Matyasek, M. Matzke, A. R. Leitch *et al.*, 2005 Preferential elimination of repeated DNA sequences from the paternal, *Nicotiana tomentosiformis* genome donor of a synthetic, allotetraploid tobacco. New Phytol. **166:** 291–303.

Slotkin, R. K., M. Vaughn, F. Borges, M. Tanurdzic, J. D. Becker *et al.*, 2009 Epigenetic reprogramming and small RNA silencing of transposable elements in pollen. Cell **136:** 461–472.

Vitte, C., and O. Panaud, 2003 Formation of solo-LTRs through unequal homologous recombination counterbalances amplifications of LTR retrotransposons in rice Oryza sativa L. Mol. Biol. Evol. **20:** 528–540.

Wang, J. L., L. Tian, H. S. Lee, N. E. Wei, H. M. Jiang *et al.*, 2006 Genomewide nonadditive gene regulation in Arabidopsis allotetraploids. Genetics **172:** 507–517.

Wawrzynski, A., T. Ashfield, N. W. G. Chen, J. Mammadov, A. Nguyen *et al.*, 2008 Replication of nonautonomous retroelements in soybean appears to be both recent and common. Plant Physiol. **148:** 1760–1771.

Wessler, S. R., 1996 Plant retrotransposons: turned on by stress. Curr. Biol. **6:** 959–961.

Wicker, T., and B. Keller, 2007 Genome-wide comparative analysis of copia retrotransposons in *Triticeae*, rice, and *Arabidopsis* reveals conserved ancient evolutionary lineages and distinct dynamics of individual copia families. Genome Res. **17:** 1072–1081.

Wicker, T., N. Yahiaoui, R. Guyot, E. Schlagenhauf, Z. D. Liu *et al.*, 2003 Rapid genome divergence at orthologous low molecular weight glutenin loci of the A and A(m) genomes of wheat. Plant Cell **15:** 1186–1197.

Witte, C. P., Q. H. Le, T. Bureau and A. Kumar, 2001 Terminal-repeat retrotransposons in miniature (TRIM) are involved in restructuring plant genomes. Proc. Natl. Acad. Sci. USA **98:** 13778–13783.

Xu, Y. H., L. Zhong, X. M. Wu, X. P. Fang and J. B. Wang, 2009 Rapid alterations of gene expression and cytosine methylation in newly synthesized *Brassica napus* allopolyploids. Planta **229:** 471–483.

Yan, L., A. Loukoianov, G. Tranquilli, M. Helguera, T. Fahima *et al.*, 2003 Positional cloning of the wheat vernalization gene VRN1. Proc. Natl. Acad. Sci. USA **100:** 6263–6268.

Yan, L., M. Helguera, K. Kato, S. Fukuyama, J. Sherman *et al.*, 2004 Allelic variation at the VRN-1 promoter region in polyploid wheat. Theor. Appl. Genet. **109:** 1677–1686.

Communicating editor: D. Voytas

GENETICS

Supporting Information
http://www.genetics.org/cgi/content/full/genetics.110.120790/DC1

Genetic and Epigenetic Dynamics of a Retrotransposon After Allopolyploidization of Wheat

Zina Kraitshtein, Beery Yaakov, Vadim Khasdan and Khalil Kashkush

DOI: 10.1534/genetics.110.120790

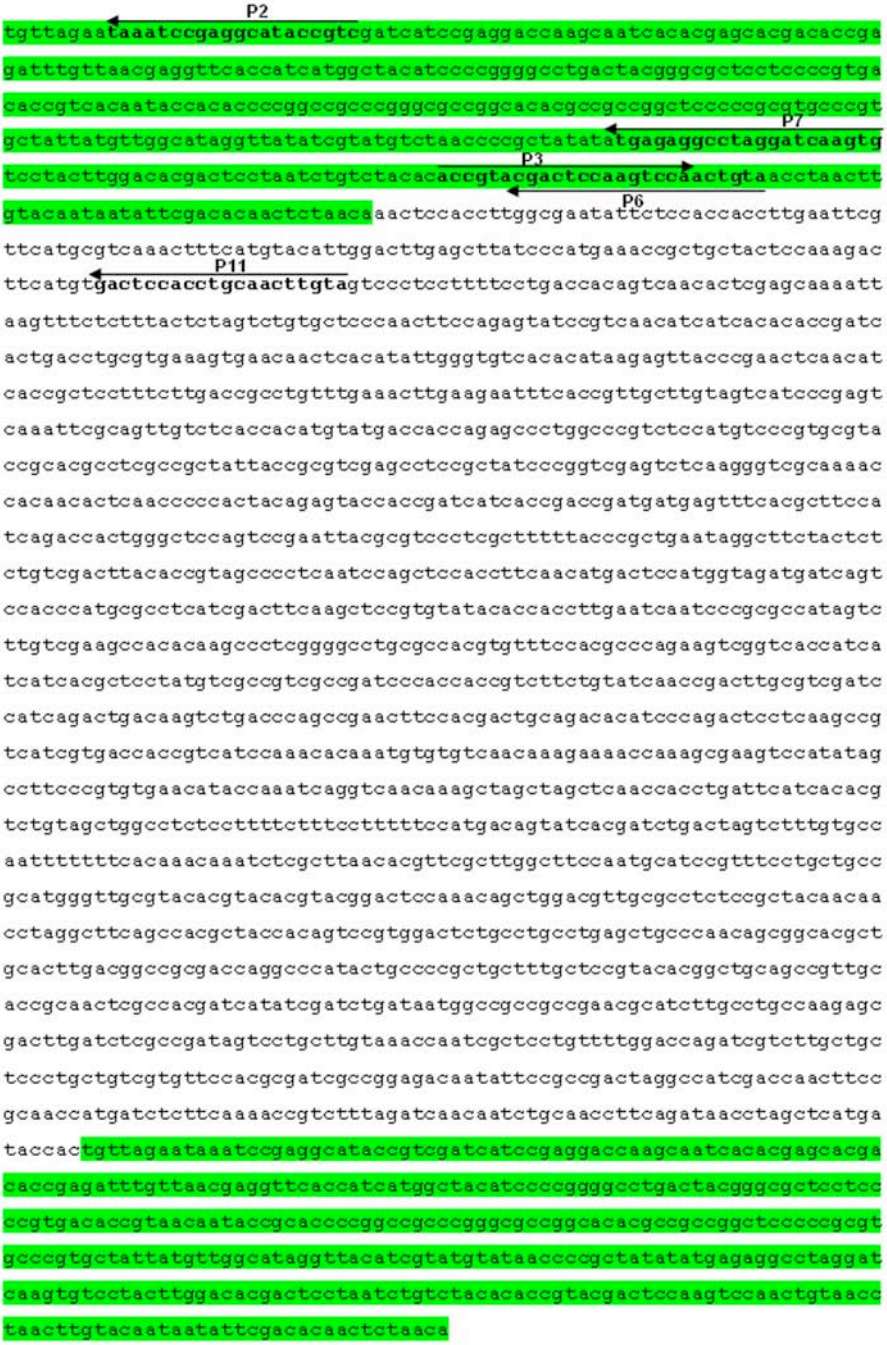

FIGURE S1.—Veju sequence (2520 bp) with its two identical LTRs (374 bp, marked in green). The positions of primers used in PCR analyses and TMD are indicated in arrows (see Table S1). The source of the sequence is accession number AF459639 (see notes in Table S1).

A.

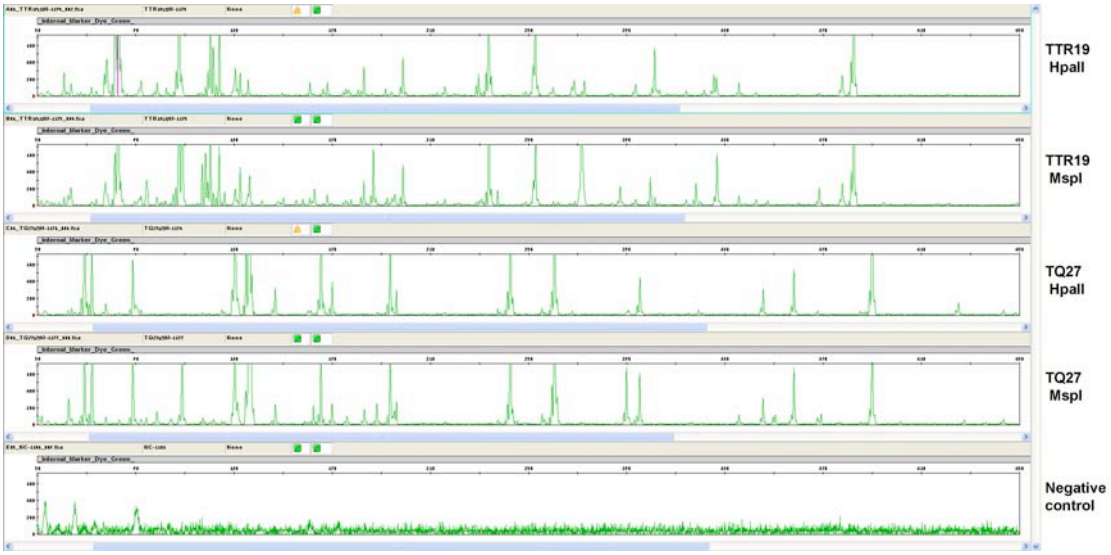
TTR19
HpaII
TTR19
MspI
TQ27
HpaII
TQ27
MspI
Negative
control

B.


Internal_Marker_Dye_Green_
TTR19
HpaII
TTR19
MspI
TQ27
HpaII
TQ27
MspI
S1
HpaII
S1
MspI
S2
HpaII
S2
MspI

FIGURE S2.—Fluorescent transposon methylation display (TMD) patterns as displayed in "GeneMapper v.4" software using P2 primer and the adapter primer, +(TACC) (P1). A. TMD patterns of *T. turgidum* ssp. *durum* (TTR19) and *Ae. tauschii* (TQ27). As a negative control, water was used as template in the PCR reaction. B. TMD patterns of *T. turgidum* ssp. *durum* (TTR19), *Ae. tauschii* (TQ27), S1 and S2 generation. Primer sequences are listed in Table S1.

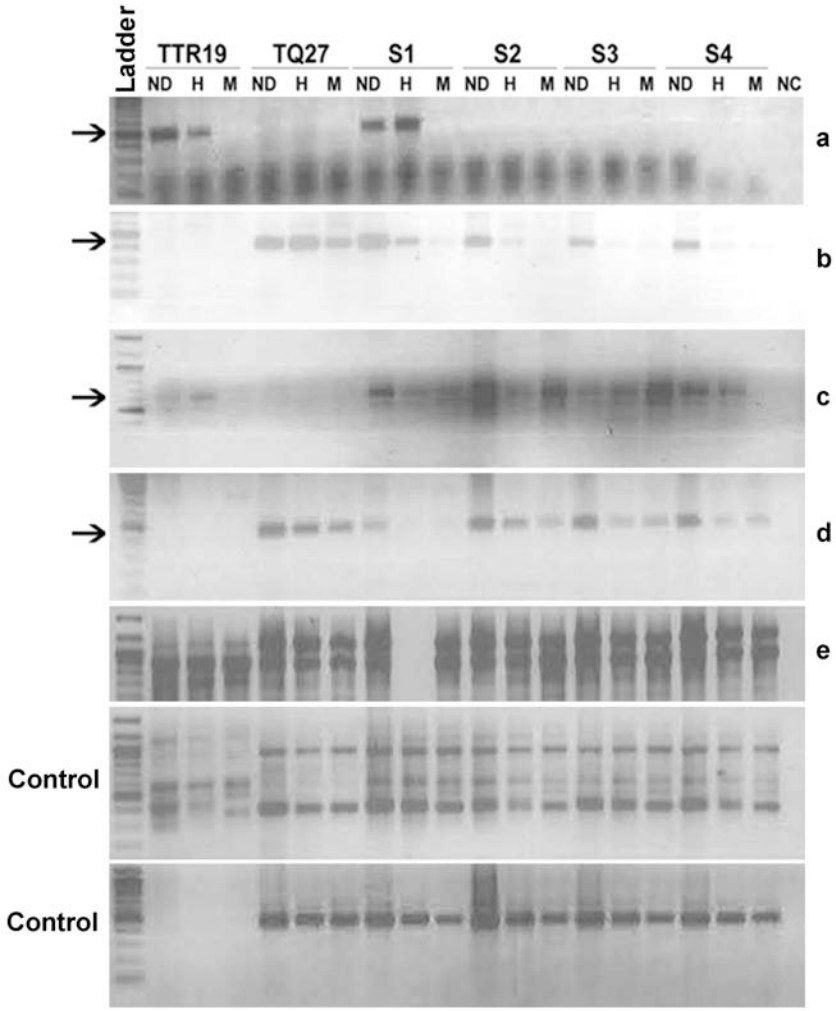

FIGURE S3.—Methylation of CCGG sites in the LTR. PCR analysis (using one primer from flanking sequences and other from LTR, see Figure 3) in leaves using undigested genomic DNA (ND) or DNA digested with either HpaII (H) or MspI (M) as the template (from parental lines and the first 4 generations of the derived allohexaploid). (a) A partially methylated *Veju* insertion in the parental line TTR19 was deleted in S2 generation. (b) A methylated *Veju* insertion in TQ27 was demethylated in S1 and subsequent generations. (c) A partially methylated *Veju* insertion in TTR19 was hypermethylated in S generations. (d) A *Veju* element underwent demthylation in S1 followed by hypermethylation in the subsequent generations. The bottom panels, where no methylation changes were seen in the newly formed allohexaploid (as seen in TMD) were used as a control for the site-specific PCR assay. As a negative control, water was used as template in the PCR reaction. A 100-bp DNA ladder (Fermentas) was used.

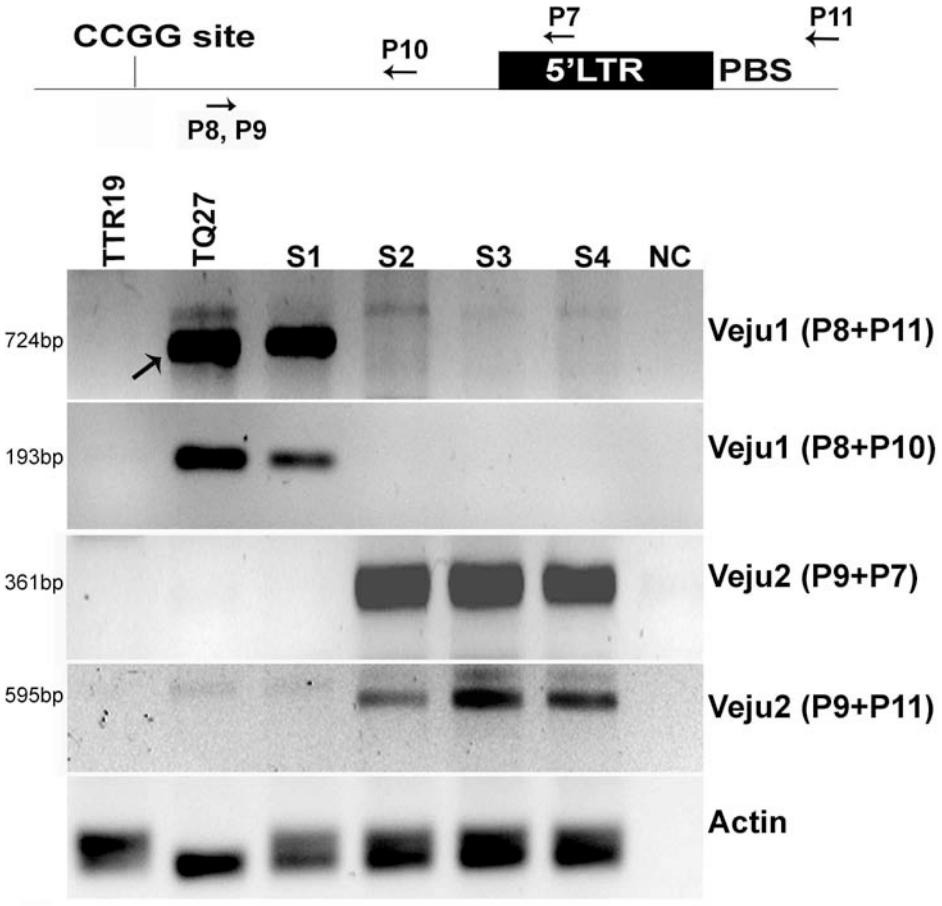

FIGURE S4.—Validation of deleted *Veju1* and new inserted *Veju2* fragments. A scheme of an LTR and flanking sequences are shown together with the primer positions used for the validation. For simplicity, the same scheme was used to show the *Veju1* and *Veju2* primer positions. For *Veju1*, PCR analysis was performed (using DNA from parental lines from the first four generations of the derived allohexaploid as template) using primer pairs P8 and P11 or P8 and P10. PCR analysis of *Veju2* was performed using primer pairs P9 and P7 or P9 and P11. Primer sequences are listed in Table S1. The size of each amplified PCR fragment (in base pairs) is indicated to the left of each panel. Actin was used for DNA quality control (see notes in Figure 3), while for a negative control, water was served as template in the PCR reaction.

If, indeed, the use of a primer from *Veju1* 5'LTR and a primer from the host flanking sequence resulted in S1 demethylation of the chimeric fragment and its elimination in subsequent generations, then the host flanking sequence should have also been eliminated. To test this hypothesis, a 193 bp segment of the host flanking sequence was amplified by PCR using primers P8 and P10. The results indeed showed that the resulting band is present in both the TQ27 (parent) and S1 generations, yet absent from subsequent generations (panel *Veju1*- P8+P10), thus indicating that the host flanking sequence had already been eliminated in S2, a process that was reproducible using independently generated S1-S4 plants (see replicates in Figure S5). The same pattern was observed using primers P8 and P11 (Figure 5), designed to amplify a 724 bp segment of a chimera that contains the host flanking sequence *Veju1* 5'LTR and an internal *Veju* sequence downstream of the 5'LTR (*Veju1*-P8+P11 panel).

For *Veju2*, The use of primers P9 and P7 (panel *Veju2*- P9+P7) produced a 361 bp PCR fragment, while the use of primers P9 and P11 (*Veju2*- P9+P11 panel) yielded a 595 bp PCR fragment. In both PCR experiments, the *Veju2*-derived band was absent in the two parental lines and the S1 generation, yet present in the S2, S3, and in S4 generations, indicating the novel insertion of *Veju2* in the S2 generation.

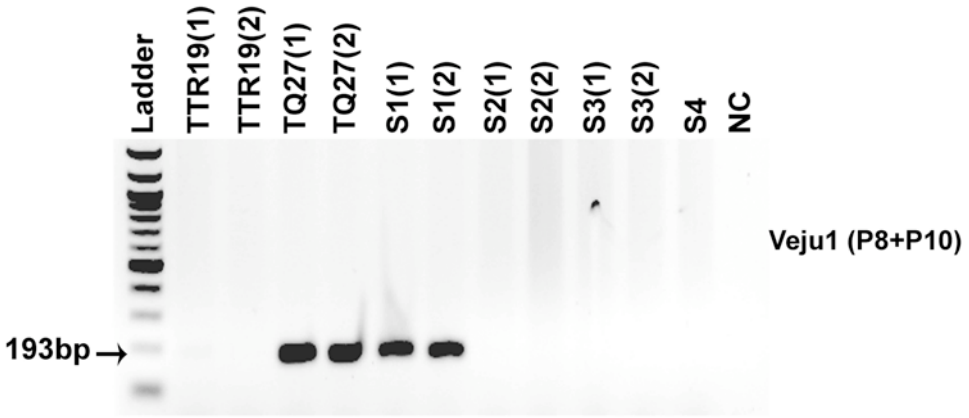

FIGURE S5.—Deletion of *Veju1* host DNA flanking sequence is repeatable. Two independent plants from parental lines TTR19, *T. turgidum* ssp. *durum* (BBAA), and TQ27, *Ae. tauschii* (DD), and from S1-S3 generations were used as templates for PCR amplification. Primers designed from *Veju1* host flanking sequence were used (P8+P10, see Figure 3 and Table S1). As a negative control (NC), water was served as a template in the PCR reaction. A 100 bp size-ladder was used.

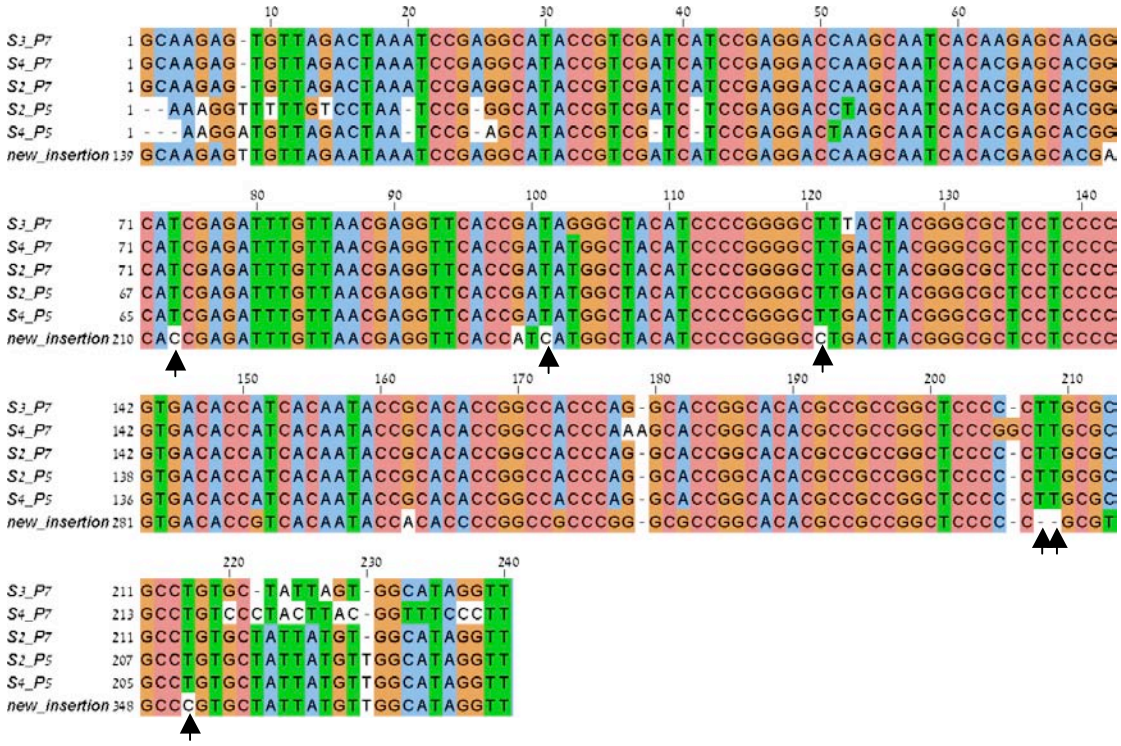

FIGURE S6.—Bisulfite sequencing of the new inserted element- *Veju2*. The bottom sequence is the bisulfite-untreated amplified sequence using P5 and P7 primers (see Figure 3) in PCR analysis. The upper 4 sequences are those new insertions isolated from S2, S3 and S4 generations following bisulfite treatment of DNA templates. The converted C to T (see arrows) indicates unmethylated cytosine. However, the unconverted cytosine indicates its methylation. The bisulfite reaction was performed using the EpiTect Bisulfite Kit (Qiagene). It is very important to mention that the efficiency of the bisulfate reaction (level of conversions from C to T) in the control sequence (unmethylated DNA, supplied in the Kit) varied between 70-80% only. Based on this, we conclude that at least 40% of the cytosines in this sequence were methylated, validated our TMD (Figure 1) and site-specific PCR results (Figure 3).

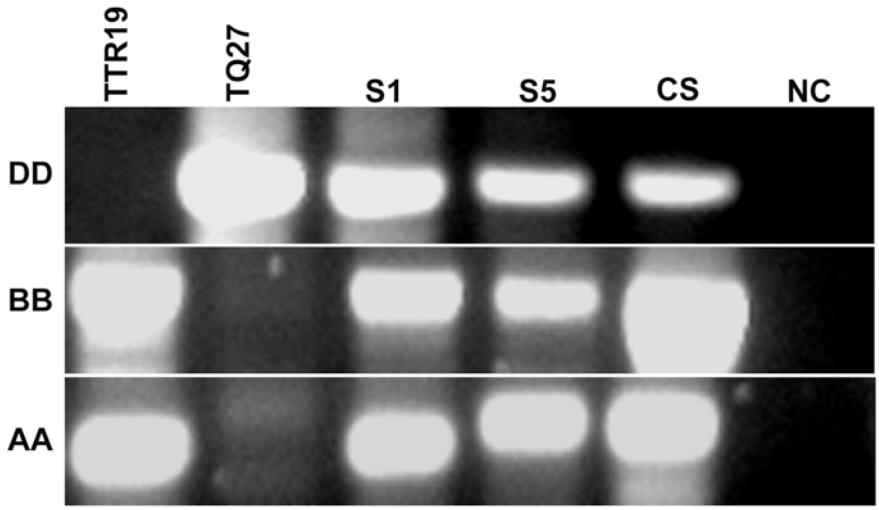

FIGURE S7.—PCR validation of *VRN1* orthologs. Genome specific primer pairs were successfully used to amplify specific orthologs from the DD, BB and AA genomes (Yan et al., 2004). Primer sequences are listed in Table S1. In addition, *VRN1* is not affected by allopolyploidization, presents in the parental lines TTR19, *T. turgidum* ssp. *durum* (BBAA), TQ27, *Ae. tauschii* (DD) and in the newly formed allohexaploid (S1 and S5 generations). *T. aestivum* (*cv.* Chinese Spring-- CS) was used as a positive control. As a negative control (NC), water was served as a template in the PCR reaction.

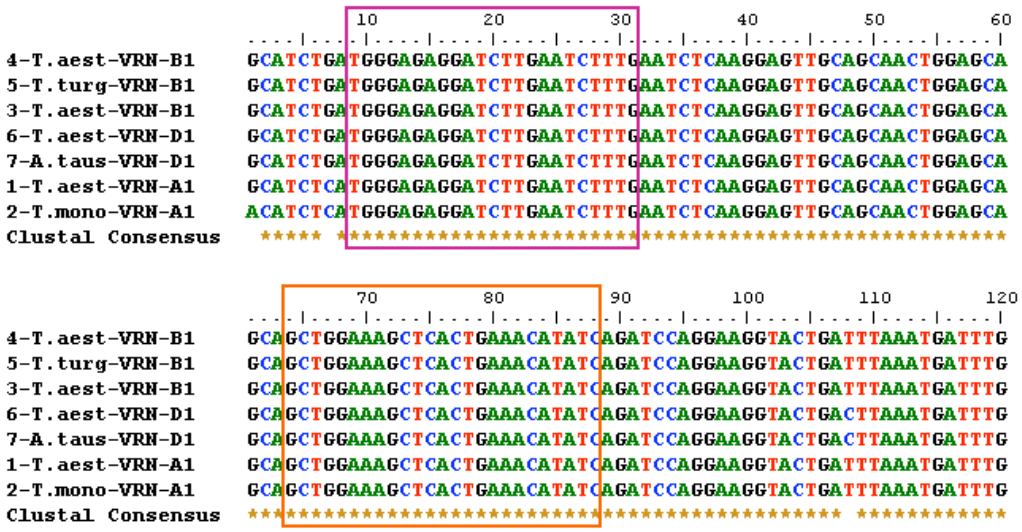

FIGURE S8.—Multiple sequence alignment of *VRN*1 orthologs. Position 1 is the beginning of exon 4. Purple and orange rectangles indicate forward and reverse primer positions, respectively, designed for qPCR analysis. The alignment includes the following wheat accessions: (1) *T. aestivum* cultivar Triple Dirk D line (AY747601.1)- *VRN*-A1 ortholog; (2) *T. monococcum* cultivar (AY244509.2)-*VRN*-A1 ortholog; (3) *T. aestivum* cultivar Triple Dirk C line (AY747604.1)- *VRN*-B1 ortholog; (4) *T. aestivum* cultivar Triple Dirk B line (AY747603.1)- *VRN*-B1 ortholog ;(5) *T. turgidum* cultivar Langdon (AY747602.1) - *VRN*-B1 ortholog; (6) *T. aestivum* cultivar Triple Dirk C line (AY747606.1)- *VRN*-D1 ortholog; (7) *A. tauschii* (AY747605.1)- *VRN*-D1 ortholog.

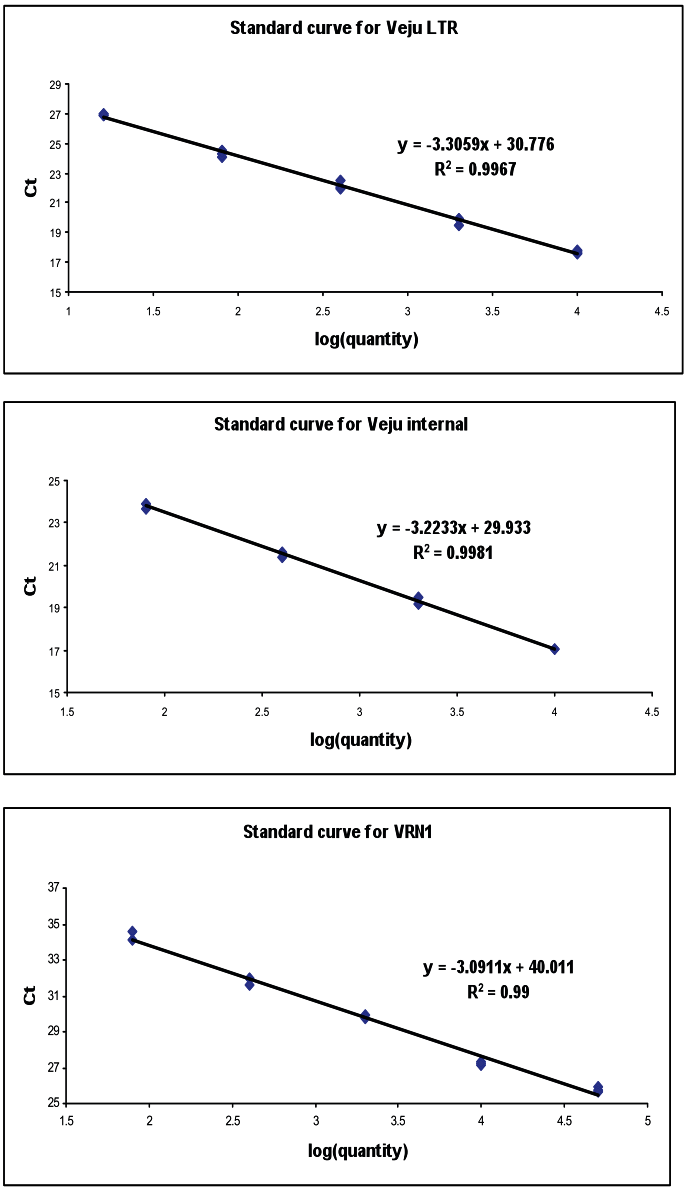

FIGURE S9.—Quality control for qPCR experiments to rule out possible competition effects in the PCR reactions. A mix of DNA templates in various concentrations was used in PCR reaction. Standard curves for *Veju*-LTR, *Veju*-internal sequence and for *VRN1* are displayed. Ct in the Y-axis indicates the cycle threshold, while the X-axis indicates the amplification quantity in *pg*. In all three cases the regression (R^2) was highly significant.

TABLE S1

List of primer sequences used for genomic PCR amplifications

Amplified sequence/ gene	Primer name[d]	Orientation	Sequence	Tm (°C)	Product Size (bp)
HpaII/ MspI adapter primer	P1	-	5'-ATCATGAGTTCCTGCTCGG-3'	59	-
MseI adapter primer	-	-	5' GATGAGTCCTGAGTAAC-3'	59	-
Veju 5' LTR[a]	P2	Reverse	5'-GACGGTATGCCTCGGATTTA-3'	59.92	-
Veju 3' LTR[a]	P3	Forward	5'-ACCGTACGACTCCAAGTCCA-3'	60.57	-
Deletion band: Validation primers	P4	Forward	5'-CAGATGCCAGAATAGCAAAG-3'	56.17	503
	P6	Reverse	5'-TACAGTTGGACTTGGAGTCG-3'	56.29	
Deletion band: Flanking region	P8	Forward	5'-CAATGCCTTTCATGCACTA-3'	58	193
	P10	Reverse	5'-TTGTGCGATTTTCTCAGTTT-3'	56.04	
Deletion band: Flanking region-internal region of *Veju*	P8	Forward	5'-CAATGCCTTTCATGCACTA-3'	58	724
	P11	Reverse	5'-TACAAGTTGCAGGTGGAGTC-3'	56.28	
New insertion band: Validation primers	P5	Forward	5'-ACAACGAGCCATCTCCAAGT-3'	59.73	304
	P7	Reverse	5'-CACTTGATCCTAGGCCTCTCA-3'	59.44	
New insertion band: Flanking region-LTR	P9	Forward	5'-TACTCCCTCCGTCCCTCCA-3'	62.95	361
	P7	Reverse	5'-CACTTGATCCTAGGCCTCTCA-3'	59.44	

New insertion band: Flanking region-internal region of *Veju*	P9	Forward	5'-TACTCCCTCCGTCCCTCCA-3'	62.95	595
	P11	Reverse	5'-TACAAGTTGCAGGTGGAGTC-3'	56.28	
Actin[b]	-	Forward	5'-GAAGCGCATATCCTTCGTAA-3'	58.02	386
	-	Reverse	5'-CCCTCTATGCAAGTGGTCGTA-3'	60.14	
VRN1 A ortholog[c]	-	Forward	5'-GAAAGGAAAAATTCTGCTCG-3'	55	480
	-	Reverse	5'-TGCACCTTCCC(C/G)CGCCCCAT-3'		
VRN1 B ortholog[c]	-	Forward	5'-CAGTACCCCTGCTACCAGTG-3'	58	1007
	-	Reverse	5'-TGCACCTTCCC(C/G)CGCCCCAT-3'		
VRN1 D ortholog[c]	-	Forward	5'-CGACCCGGGCGGCACGAGTG-3'	60	792
	-	Reverse	5'-TGCACCTTCCC(C/G)CGCCCCAT-3'		

[a]Primers were designed from accession number AF459639.
[b]Primers were designed from accession number AF326781
[c]Primers were designed as described (Yan et al., 2004).
[d]Primer names are given based on their appearance in the figures.

TABLE S2

List of primer sequences used for qPCR amplifications

Amplified sequence/ Gene	Primers			Standard curve		
	Orientation	Sequence	Primer express Tm (°C)	Slope[c]	PCR Efficiency (%)	$R^{2(d)}$
*VRN*1[a]	Forward	5'-TGGGAGAGGATCTTGAATCTTTG-3'	58.3	-3.274	102.035	0.997
	Reversed	5'-GATATGTTTCAGTGAGCTTTCCAGC-3'	59.3			
Veju's internal sequence[b]	Forward	5'-TCGAGTCTCAAGGGTCGCA-3'	59	-3.236	103.702	0.993
	Reversed	5'-TGGTCTGATGGAAGCGTGAA-3'	59			
Veju's LTRs[b]	Forward	5'-TCGATCATCCGAGGACCAAG-3'	60	-3.476	93.956	0.995
	Reversed	5'-GCCATGATGGTGAACCTCGT-3'	59			

[a] Primers were designed according to ClastalX multiple sequence alignment (see Figure S8).

[b] Primers were designed from accession number AF459639.

[c] Indicates primer efficiency, where primers are efficient in slope of -3 to -3.6.

[d] R^2 from 0.98-0.99 indicates an ideal primer efficiency.

TABLE S3

Number of TMD bands amplified in the parental lines *T. turgidum* ssp. *durum* (TTR19) and *Ae. tauschii* (TQ27) and in the first four generations (S1-S4) of the derived allohexaploid.

Parental lines	Total number of TMD bands[a]	Number of polymorphic bands (%)[b]	Total number of changes in S1-S4 (%)[c]
TTR19	559	231 (41.3)	
TQ27	330	132 (40.0)	486 (54.6)
Total	889	361 (40.6)	

[a]Monomorphic bands in H (*HpaII*) and M (*MspI*) lanes were scored only once.

[b]Polymorphic bands between H and M lanes indicate the level of methylation (%) in the parental lines.

[c]Any bands showing deviation from additivity of the parental lines in at least one of the S generations was scored as a change in the allohexaploid. The level (%) of changes in TMD patterns from the number of total bands of both parents (TTR19+TQ27) is shown.

TABLE S4

Examples of TMD patterns of bands that altered in the amphipoid

Type of alteration	TMD pattern[a]											
	TTR19		TQ27		S1		S2		S3		S4	
	H	M	H	M	H	M	H	M	H	M	H	M
Methylation alteration	-	+	-	+	-	+	-	+	-	+	+	+
	+	+	+	+	+	+	+	-	+	-	+	-
	-	-	+	+	-	-	+	+	+	+	+	+
	-	-	-	+	-	-	-	+	-	+	-	+
	-	-	+	+	-	-	-	+	-	+	-	+
	+	-	+	-	-	-	+	-	+	-	+	-
	-	+	-	-	-	-	-	+	-	+	-	+
	+	-	+	+	+	-	+	-	+	-	+	-
	-	-	+	+	+	-	+	-	+	-	+	-
	-	-	+	+	+	-	+	-	+	-	+	-
	-	-	+	-	-	-	+	-	+	-	+	-
Methylation alteration in S1 or S2 followed by absence of bands	-	-	+	-	+	+	-	-	-	-	-	-
	+	+	+	+	+	-	-	-	-	-	-	-
	-	-	+	+	-	-	+	+	-	-	-	-
Absence of bands in S1 or S2	-	-	+	+	+	+	-	-	-	-	-	-
	-	-	-	+	-	-	-	-	-	-	-	-
	+	+	-	-	+	+	-	-	-	-	-	-
	+	+	-	-	+	+	-	-	-	-	-	-
	-	-	+	+	-	-	-	-	-	-	-	-
	-	-	+	+	-	-	-	-	-	-	-	-
	-	-	-	+	-	-	-	-	-	-	-	-
	+	+	-	-	+	+	-	-	-	-	-	-
	-	+	-	-	-	-	-	-	-	-	-	-
	-	-	+	-	-	-	-	-	-	-	-	-
	+	+	-	-	+	+	-	-	-	-	-	-
	+	+	-	-	-	-	-	-	-	-	-	-
	-	-	+	-	-	-	-	-	-	-	-	-
	-	-	-	+	-	-	-	-	-	-	-	-
	-	-	-	+	-	-	-	-	-	-	-	-
	-	-	+	-	-	-	-	-	-	-	-	-
	-	-	+	+	-	-	-	-	-	-	-	-
	-	-	+	+	-	-	-	-	-	-	-	-
	-	-	+	-	-	-	-	-	-	-	-	-
Appearance of novel bands in S2	-	-	-	-	-	-	+	-	+	-	+	-
	-	-	-	-	-	-	+	+	+	+	+	+

[a] +, band present; -, band absent. H notes HpaII lane and M notes MspI lane (See Figure 1).

TABLE S5

Characterization of 10 of the altered TMD fragments in newly formed allohexaploid

Clone ID.	Size(bp)	Sequence similarity[b]	TMD pattern[a]												Primer combination[d]
			TTR19		TQ27		S1		S2		S3		S4		
			H	M	H	M	H	M	H	M	H	M	H	M	
Z531	229	Unknown	+	+	-	-	-	-	+	+	+	+	+	+	P1-TCAG + *Veju* 5' LTR
Z541	188	Unknown	-	-	+	+	-	-	+	+	+	+	+	+	P1-TCAG + *Veju* 5' LTR
Z573	160	Unknown	-	-	+	+	-	-	-	+	-	+	-	+	P1-TCAG + *Veju* 5' LTR
Z534	193	Unknown	-	-	+	+	-	-	+	+	-	-	-	-	P1-TCAG + *Veju* 5' LTR
Z527	248	Unknown	+	+	-	-	+	+	-	-	-	-	-	-	P1-TCAG + *Veju* 5' LTR
Z564	178	Unknown	-	-	+	+	-	-	-	-	-	-	-	-	P1-TCAG + *Veju* 5' LTR
Z581	133	EST-CD888659	+	+	-	-	+	+	-	-	-	-	-	-	P1-TCAG + *Veju* 5' LTR
Z530 (*Veju1*)[c]	311	EST-CJ569351	-	-	+	-	-	-	-	-	-	-	-	-	P1-TCAG + *Veju* 5' LTR
Z623	155	Unknown	-	-	+	+	-	-	-	-	-	-	-	-	P1-TCAG + *Veju* 3' LTR
Z572(*Veju2*)[c]	173	Unknown	-	-	-	-	-	-	+	+	+	+	+	-	P1-TCAG + *Veju* 5' LTR

[a](+), band present ; (-), band absent.

[b]No significant sequence hits in databases at e-value.

[c]See text (results) for more details.

[d]See details in Table S1. The four additional nucleotides to the adaptor primer (P1, see Table S1) note the selective nucleotides in the selective PCR in TMD reaction.

TABLE S6

Sequences of the 10 TMD fragments (see Table S5)

Clone	Sequence[a]
Z531	CATGAGTCCTGCTCGGTCAGGGAGTAGCAAGCTTAATTAGGCATGCCTCTCTCCGTAGAGCGAAAACCGTGCATGGCTCCAAATGAGGTGCCATGCACCAAAAAGGACAAACAAT AACGAGAACTATATATAGAGAGAGAAAATTGAAGTAAAGTTGAGAATCAGAGGACACGGTTGGGGAAGGTGCATGTAGATGCTCATTGTTAGAATAAATCCGAGGCATACCGTC
Z541	CATGAGTCCTGCTCGGTCAGGGGCTTACCTAGCAAGATGATGACCTATTTGCACCTGCAACCCAAGTTGTGTGATGGGTTTTATCATTTTACAAGTTATGTGATTAAAGTG CACCCATCGGACAAATTCTAGGATCGCTAGACGCCAGTGTCATTTACTCTGTTAGAATAAATCCGAGGCATACCGTC
Z573	CATGAGTCCTGCTCGGTCAGTCCATGCGACCACACGCCGCCGATTCCGATTAGTCCTTGCACGTCGCCAGATTTCGCCGATAGCTTCGTGTTCTCCTTCCTCTAGATCGACGGAA CCGCAACCTCTTCGATCCTTGCTCAGGATACCACTTGTTAAAATAAATCCGAGGCATACCGTC
Z534	CATGAGTCCTGCTCGGTCAGATTGCTGAGGGACCTGTTACTTTCAGTGCTGGGAATTAGTTAAAAGTGTAACCTAACTTTTCTCTATCGGTCCTGCTGCATATGCTCCTGTCCCTTT CCAGCCTCTGCTCTACTGAGTACTGACTGAGTCAAACTGATCAGCAAGTGTTAGAATAAATCCGAGGCATACCGTC
Z527	CATGAGTCCTGCTCGGTCAGTGGCCCAAATAAGGCGAAACAAAGTATTATTACTTCCAAATCCTTACAAAATGTTCCTATCATGCATGTTTGGTTTGTAGTACTGCAAACCATATGTT TGTTCCTATAAAGTTTTCCTGTCACTCCAAATTTCCATTCGGTCCAGGCTCGTCGAGAAGTCCATAAGTTTTTAAATCCTTCGAAAAAAGTTCTTGTGTCTTTGTTAGAATAAATCCG AGGCATACCGTC
Z564	CATGAGTCCTGCTCGGTCAGTCCATGCGACCACACGCCGCCGATTCCGATTAGTCCTTGCACGTCGCCAGATTTCGCCGATAGCTTCGTGTTCTCCTTCCTCTAGATCGACGGAA CCGCAACCTCTTCGATCCTTGCTCAGGATACCACTTGTTAAAATAAATCCGAGGCATACCGTC
Z581	CATGAGTCCTGCTCGGTCAGCGGGGATGCTACAGGTCTATCAAGATGGCCAACACGACACATCGGCGGCGGCGTGTCGGATGGCCTCGCCGTTGACCGTTTAATATGTTAGAATT AAATCCGAGGCATACCGTC
Z530 (*Veju1*)	CATGAGTCCTGCTCGGTCAGGTGACATACACTGATACACTACAGCTGATCCCGTTCATCCCCAACCGGGCAATGCCTTTCATGCACTAATGATGAATCTTGTTCTTTATCCACCAT CCAGATGCCAGAATAGCAAAGTCTTTAGGAGAACAACACTGGAGTATGTGAGTTCGAGAAGGTTGTTCTTTATCCCCCATCTAGATGCTTAGATCCTCCAAACCCATCCTCCAACT ATCATGAGATAAACTGAGAAAATCGCACAAAAAGATAACGTTGGTGTGTTGTGTTAGAATAAATCCGAGGCATACCGTC
Z623	CATGAGTCCTGCTCGGTCAGACAGACGAGATACGACCGATCGAGTGCAAGCAGGGTGATCGATCGACAAGAAGAGGAAGGACGATGGGCATGGTTAGAGTTGTGTCGAATATTA TTATACAAGTTAGGTTACAGTTGGACTTGGAGTCGTACGGT
Z572(*Veju2*)	CATGAGTCCTGCTCGGTCAGATGAGACATCTATAGACTATAGTAGTAGTTGTATAACCAAATACTCCCTCCGTCCCTCCATCTTATTGGTCCAGAGTTAGCATCGGCCGGGCTTCT TTACAACGAGCCATCTCCAAGTGCAAGAGTGTTAGACTAAATCCGAGGCATACCGTC

[a] *Veju* LTR sequence is indicated in red and flanking host sequences indicated in black. In addition, *Veju* LTR primer is marked in green and H/M adaptor primer is marked in yellow.